



UNIVERSIDADE FEDERAL DE RORAIMA
PRÓ-REITORIA DE PESQUISA E PÓS-GRADUAÇÃO
PROGRAMA DE PÓS GRADUAÇÃO EM RECURSOS NATURAIS
MESTRADO EM RECURSOS NATURAIS

BRUNA MENDEL NAISSINGER

**CONTROLES ABIÓTICOS DE UMA SAVANA AMAZÔNICA:
UMA ABORDAGEM DE SENSORIAMENTO REMOTO MULTISENSOR**

BOA VISTA, RR
2022

BRUNA MENDEL NAISSINGER

**CONTROLES ABIÓTICOS DE UMA SAVANA AMAZÔNICA:
UMA ABORDAGEM DE SENSORIAMENTO REMOTO MULTISENSOR**

Dissertação apresentada ao Programa de Pós-graduação em Recursos Naturais da Universidade Federal de Roraima, requisito parcial para a obtenção do grau de Mestra em Ciências Ambientais, na área de concentração: Manejo e Conservação de Bacias Hidrográficas.

Orientador: Prof. Dr. Stélio Soares Tavares Júnior.

Coorientador: Prof. Dr. Pedro Aurélio Costa Lima Pequeno.

BOA VISTA, RR
2022

Dados Internacionais de Catalogação na publicação (CIP)
Biblioteca Central da Universidade Federal de Roraima

N158c Naissinger, Bruna Mendel.

Controles abióticos de uma savana amazônica : uma abordagem de sensoriamento remoto multisensor / Bruna Mendel Naissinger. – Boa Vista, 2022.

81 f. : il.

Orientador: Prof. Dr. Stélio Soares Tavares Júnior.

Coorientador: Prof. Dr. Pedro Aurélio Costa Lima Pequeno.

Dissertação (mestrado) – Universidade Federal de Roraima,
Programa de Pós-Graduação em Recursos Naturais.

1 – Bacia Sedimentar do Tacutu. 2 – Radar de abertura sintética. 3 – MLME. 4 – SEM. I – Título. II – Tavares Júnior, Stélio Soares (orientador). III – Pequeno, Pedro Aurélio Costa Lima (coorientador).

CDU – 556.51(811.4)

BRUNA MENDEL NAISSINGER

**CONTROLES ABIÓTICOS DE UMA SAVANA AMAZÔNICA:
UMA ABORDAGEM DE SENSORIAMENTO REMOTO MULTISENSOR**

Dissertação apresentada como pré-requisito para conclusão do Curso de Mestrado em Ciências Ambientais (Recursos Naturais) da Universidade Federal de Roraima, defendida em 12 de maio de 2022 e avaliada pela seguinte Banca Examinadora:

Documento assinado digitalmente
 STELIO SOARES TAVARES JUNIOR
Data: 29/08/2022 11:00:32-0300
Verifique em <https://verificador.iti.br>

Prof. Dr. Stélio Soares Tavares Júnior

Orientador - Universidade Federal de Roraima UFRR

Documento assinado digitalmente
 TATIANA MORA KUPLICH
Data: 02/09/2022 11:38:14-0300
Verifique em <https://verificador.iti.br>

Profa. Dra. Tatiana Mora Kuplich

Membra – Instituto Nacional de Pesquisas Espaciais INPE



Reinaldo Imbrozio Barbosa
Assessor Titular
INPA/Roraima

Prof. Dr. Reinaldo Imbrozio Barbosa

Membro – Instituto Nacional de Pesquisas da Amazônia INPA

Documento assinado digitalmente
 LUIZA CAMARA BESSERA NETA
Data: 29/08/2022 11:04:54-0300
Verifique em <https://verificador.iti.br>

Profa. Dra. Luiza Câmara Beserra Neta

Membra – Universidade Federal de Roraima UFRR

Às meninas, futuras cientistas, dedico.
Questionem. Ocupem.
Resistam!

AGRADECIMENTOS

Às políticas de esquerda que me permitiram chegar até aqui, a despeito de viver no país das desigualdades. Ao auxílio financeiro recebido pela Coordenação de Aperfeiçoamento de Pessoal de Nível Superior - CAPES, um privilégio em uma gestão marcada por tantos cortes e retrocessos.

Aos orientadores Stélio Tavares e Pedro Pequeno. Agradeço a liberdade e a confiança na escolha da temática e na execução desta pesquisa. Pedro, obrigada por me ensinar a usar o R, pelo estímulo na biogeografia e pela oportunidade de ser monitora nas disciplinas de estatística. À UFRR e ao PRONAT pela infraestrutura. Aos professores do PRONAT, em especial aos professores da banca de qualificação Carolina Castilho, Haron Xaud, Luiza Bezerra Neta e Marcia Falcão pelas sugestões. Agradeço também ao professor Frutuoso pelos esclarecimentos em relação aos solos da savana.

Aos colegas do PRONAT, em especial às queridas e competentes: Flávia Pinheiro e Rachel Pinho, que recorro frequentemente com dúvidas sobre a vida, o universo, o lavrado e tudo o mais. À turma de 2019, foram seis de meses de muito convívio, seminários, conversas e descobertas! Seguidos da pandemia, de isolamento e de muitas perdas: fica à memória, o colega Raphael Amorim.

Ao INPE e à UFRGS pela oportunidade de cursar disciplinas do sensoriamento remoto, especialmente aos professores que as ministraram: Camilo Renno, Claudio Barbosa, Evelyn Novo, Eymar Lopes, Fabio Gama, Gilberto Queiroz, Jose Mura, Lênio Galvão, Sidnei Sant Anna, Tatiana Kuplich, Thales Korting e Yosio Shimabukuro. Aos colegas do Muro das Lamentações: Karol, Mario, Maíra, Tânia e Philipe.

Ao professor Gustavo Baptista do Fascinante Mundo do Sensoriamento Remoto, por fazer jus ao nome da sua comunidade, obrigada pela didática e pela ajuda com o modelo linear de mistura espectral, à professora Milena Andrade também da comunidade, pela atenção acerca das áreas de inundação. Ao pesquisador Carlos Cordeiro, pela cordialidade e referências indicadas. À pesquisadora Marina Fagundes pela boa vontade e disposição em explicar vegetação para a geóloga aqui, à Carmem Vieira pelas dicas sobre os solos. Ao professor Jonas Souza, da UFPB, por disponibilizar suas aulas sobre geomorfologia

fluvial no *youtube*, meu *podcast* favorito durante os meses de processamento das imagens.

À Milena Escarrone e ao efeito borboleta. À Tainara Ximenes, irmã que o multiverso me deu e a quem os agradecimentos devidos transcendem o espaço das palavras. Ao Neto Freitas e ao seu otimismo avesso ao meu, por jurar que a chuva está passando enquanto a estrada se transfaz em cachoeira. À Zaya, tão pequena já transbordando arte e personalidade e à maravilha que é ver crescer essa gaiata incrível, esperta, malandra e mimada de sua titia. Ao Vladimir de Souza, à Vera Soares e aos seus meninos pela acolhida em Boa Vista e por serem sempre tão camaradas e solícitos. Aos amigos de longe, por se manterem por perto: Demétrius Lima, Niege Borges, Mara Tedesco, Tuta Freitas, Mai Vergara, Antônio Antqueira e Eduardo Aguiar.

À minha mãe, Melania Mendel, guerreira, determinada e incansável em lutar pela gente contra todas as probabilidades, por defender e priorizar visceralmente minha educação, apesar de ter sido privada da sua. Aos meus irmãos que admiro, respeito e quero muito bem: Jeferson Mendel, sempre humilde e prestativo, com quem compartilho as boas memórias da infância, parceiros de taco, carreta de lomba, bolinhas de gude, banhos de chuva, colecionadores de álbuns de figurinhas, exímios arrecadadores de balas do papai noel, e Caroline Mendel, minha irmãzinha ainda ontem tão pitoca, doce, sorridente, que de repente cresceu tão descolada, me tomado de orgulho, linda, feminista, designer gráfica, ilustradora, obrigada por arrumar a figura do perfil esquemático dos solos/geologia e pelos pitacos de sempre nas cores e caras dos meus mapas e é claro, por zoar minhas fotos de “eu e as pedras, as pedras e eu”. À minha família: Guga e os gatos. Guga, por partilhar a vida e cada etapa deste trabalho comigo, pelas intermináveis conversas e confidências e por ser lindo, te amo meu amor! Aos nossos nenês gatos: Haroldo, Aurora, Galileu e Benedito - os mais fofos, ronronentes, queridos, carinhosos, cheirosos, peludinhos, e companheirinhos do universo!

Ao lavrado, cuja existência desconhecia até iniciar este mestrado, pelo seu intrigante e desafiador mosaico de unidades, no qual estive mergulhada nesses últimos dois anos e meio. Saio dessa imersão com um novo e curioso olhar às ciências ambientais e à evolução das paisagens.

que entre raiz e flor há um breve traço:
o silêncio do lenho,
entre a raiz e a flor, o tempo e o espaço.

(Jorge de Lima)

RESUMO

Savanas sustentam grande biodiversidade e altos níveis de endemismo de espécies, ocorrendo em todo o mundo, inclusive em meio à densa floresta Amazônica. Funcionam como áreas de recarga da bacia hidrográfica Amazônica, que, dada a dimensão continental, exerce um papel central no ciclo hidrológico. A despeito dessa importância, a saúde ecológica desses ecossistemas está ameaçada pela expansão do agronegócio e pelo avanço do aquecimento global. Os parâmetros que controlam a distribuição das savanas na Amazônia, em larga escala, ainda são poucos conhecidos. Este trabalho apresenta a verificação e a quantificação dos controles diretos e indiretos de variáveis abióticas na atividade fotossintética da vegetação, representada pelo Índice de Vegetação por Diferença Normalizada (NDVI) em uma série temporal de 5 anos, em um recorte que engloba a Bacia Sedimentar do Tacutu no Brasil, cuja origem e deposição está associada à evolução das Savanas da Guiana. As variáveis abióticas utilizadas foram litologias (rochas), formas de relevo, altitude, declividade, clima (precipitação e temperatura), frequência de inundação e parâmetros dos solos: Capacidade de Troca Catiônica (CTC), Estoque de Carbono Orgânico (ECO), Densidade Aparente e Percentual de Areia. Uma análise confirmatória de Modelagem de Equações Estruturais (SEM) foi aplicada para investigar as relações causais hipotéticas em um diagrama de caminhos. Nove imagens multiespectrais Sentinel-2 de 2017 a 2021, imagens de radar ALOS PALSAR e o modelo digital de elevação NASADEM foram utilizados para construir a frequência de inundação e a forma do relevo das planícies fluviais por meio do Modelo Linear de Mistura Espectral (MLME) e da fusão de imagens ópticas e de imagens de Radar de Abertura Sintética (SAR) em softwares livres. Os resultados mostraram que o NDVI variou 60% entre os períodos secos e úmidos. A configuração atual da paisagem, expressa predominantemente pela Formação Sedimentar Boa Vista e os produtos de seu retrabalhamento, dispostos em longas superfícies de aplainamento, resultantes de ciclos sucessivos de erosão e deposição, pontuado por relevos residuais (inselbergs) afetam indiretamente o NDVI, isto é, rochas e formas de relevo afetam os solos, que afetam o NDVI. As variáveis com efeito direto explicaram 48% da variação no NDVI, sendo que a densidade aparente teve o maior efeito devido à presença de horizontes coesos que dificultam o estabelecimento de raízes e a drenagem da água nos solos. Os indicadores de

fertilidade (CTC e ECO) tiveram efeito negativo porque os solos são ácidos e com alto teor de alumínio permutável. O efeito da precipitação é positivo, e o efeito da frequência de inundação é negativo, sendo essas restrições hidroedáficas evidenciadas também pelo efeito positivo da concentração de areia nos solos. Essa abordagem demonstrou a relevância da evolução da paisagem, dos solos e do clima na distribuição espacial e temporal da cobertura vegetal.

Palavras-chave: Bacia Sedimentar do Tacutu. Radar de Abertura Sintética. MLME. SEM.

SUMÁRIO

1	INTRODUÇÃO	11
2	ARTIGO: ABIOTIC DRIVERS IN AN AMAZON SAVANNA USING MULTISENSOR REMOTE SENSING.....	18
2.1	NORMAS DA REVISTA	75
3	CONCLUSÃO	76
	REFERÊNCIAS.....	78

1 INTRODUÇÃO

Savanas ocorrem pela complexa interação de processos bióticos, abióticos e antrópicos. No âmbito global, os principais controles são: água, fogo, solos, clima, herbivoria, coexistência, competição e facilitação de espécies e a história evolutiva das paisagens (LEHMANN et al., 2011). São compostas por um mosaico de distintas formações vegetais, reconhecidas pela alta razão entre espécies herbáceas e espécies arbóreas, alta riqueza de espécies herbáceas em pequena escala, alto endemismo, banco de sementes transiente, brotos persistentes, alta biomassa subterrânea, pouca acumulação de liteira e dosséis descontínuos e abertos (VELDMAN et al., 2015). O clima em que se desenvolvem é caracteristicamente seco durante praticamente metade do ano e bastante úmido durante a outra metade. O alto grau de endemismo e biodiversidade das savanas está associado aos padrões de herbivoria e de alterações do solo provocados pela fauna local, ao pastoreio de baixa intensidade, à existência de solos rasos, oligotróficos e com altas e por vezes tóxicas concentração de metais, bem como ao déficit hídrico sazonal e à ocorrência de incêndios naturais (VELDMAN et al., 2015). Estes dois últimos fatores acabaram por selecionar uma flora xerofítica, ou seja, adaptada às secas e incêndios através de xeromorfias como cascas, cutículas ou células epiteliais espessas, presença de sílica e/ou tricomas na epiderme, folhas hipoestomáticas, estômatos com cristas, mesófilos dorsiventrais, colênquima e feixes vasculares (MISTRY; BERADI, 2000; SIMIONI et al., 2017).

Embora raro, o fogo pode ocorrer de forma natural em paisagens savânicas durante a estação seca, principalmente porque as gramíneas proporcionam imensas quantidades de matéria orgânica altamente combustível quando desidratadas (BARBOSA; FEARNSIDE, 2005a,b; BARNI et al., 2015). Por esta razão, costuma-se dizer que as savanas são um tipo de vegetação à prova de fogo, porém, este é um mal entendido. Apesar das savanas terem experimentado incêndios naturais desde milhões de anos antes da chegada dos seres humanos, a escala e frequência dos incêndios antropogênicos nos últimos anos estão além da capacidade de resiliência das savanas. Esses incêndios têm resultado em sua desestruturação e perda de equilíbrio fitossociológico, principalmente de seu componente ripário (FLORES et al., 2021; GOMES et al., 2020).

As savanas brasileiras caracterizam-se por apresentar vegetação xeromórfica de clima estacional (períodos de seca e de chuvas) ou, mais raramente, ombrófilo, disposta em solos bastante lixiviados, oligotróficos, aluminotóxicos, com sinúsias de hemicriptófitos, geófitos, fanerófitos de pequeno porte (IBGE, 2012). O Sistema Brasileiro de Classificação da Vegetação reconhece dois tipos savânicos, as savanas propriamente ditas e as savanas estépicas, ambas podem ser subdivididas em Savana Florestada, Savana Arborizada, Savana Parque e Savana Gramíneo-Lenhosa (IBGE, 2012). Na região amazônica, as savanas se fazem presentes quer como grandes e contínuas áreas, quer como pequenas e descontínuas manchas, perfazendo cerca de 5% dos quase 6 milhões de km² do bioma amazônico (CARVALHO; MUSTIN, 2017; PENNINGTON; LEHMANN; ROWLAND, 2018). Elas são o lar de cerca de 40 espécies de plantas produtoras de sementes exclusivas do Brasil (DEVECCHI et al., 2020).

Muitos incêndios têm substituído a floresta amazônica por uma vegetação graminosa monoespecífica, que não deve ser confundida com a vegetação de savana, pois esta é mais complexa florística e estruturalmente (VELDMANN; PUTZ, 2011; HOEVE et al., 2012). Por muito tempo acreditou-se que as savanas amazônicas seriam o resultado do avanço de savanas externas (dos Llanos ao norte e do Cerrado ao sul) para os espaços deixados pela floresta amazônica quando esta recuava durante episódios glaciais quaternários. Entretanto, evidências recentes indicam uma origem autóctone, pois elas já estavam presentes no bioma amazônico muito antes do quaternário e há mais similaridade genética e florística dos elementos das savanas amazônicas entre si, do que entre eles e seus vizinhos externos (VELOSO et al., 1975; DEVECCHI et al., 2020; RESENDE-MOREIRA et al., 2018).

A Savana da Guiana, situada na fronteira entre a Guiana, a Venezuela e o Brasil, é a segundo maior área de savana do Bioma Amazônico, totalizando 68145 mil km² (BARBOSA; CAMPOS, 2011). Aproximadamente 62% dessa área está no Brasil, no estado de Roraima, onde é conhecida por “Lavrado”, configurando-se na maior porção contínua de savana amazônica do país. Em Roraima, a divisão entre savana e savana estépica é mais geográfica do que fitofisionômica (Miranda e Absy, 2000), sendo reconhecidos para ambos os tipos de savana os subtipos Savana Arbórea Florestada, Savana Arbórea Aberta, Savana Parque e Savana Graminosa, podendo ou não apresentarem Matas de Galeria, Manchas de Floresta e Veredas de

Palmeiras, destacando-se as veredas de *Mauritia flexuosa* (Buritizais) ao longo de muitos igarapés (VELOSO et al., 1975; BARBOSA; MIRANDA, 2005; BARBOSA et al., 2007).

O interesse científico pelas savanas tem crescido principalmente pelo fato de serem importantes focos de biodiversidade e por albergarem inúmeras espécies endêmicas, mas também pelo reconhecimento de que são importantíssimas zonas de recarga de aquíferos e estabilização de regimes hídricos superficiais (MILLER et al., 2012; VILLALOBOS-VEGA et al., 2014; CARVALHO; MUSTIN, 2017; FURLAN et al., 2020). A despeito de toda essa importância, as savanas do mundo têm sido alvo de crescente e predatória pressão exploratória e no Brasil a situação não é diferente (VACCHIANO et al., 2019). Dentre os problemas que assolam as savanas é possível citar a perda ou exclusão de espécies, a desestruturação, fragmentação de habitats e comunidades nativas e a perda de tipos funcionais, cujas causas principais são as mudanças antrópicas nos padrões de uso e cobertura do solo, a introdução de espécies exóticas, o sobrepastoreio, a contaminação dos solos e águas subterrâneas por nitritos e nitratos de fertilizantes e compostos orgânicos nocivos de agrotóxicos, a intensificação dos regimes de fogo, a exploração irracional dos recursos hídricos e as mudanças climáticas globais (OSBORNE et al., 2018). Dentre os principais agentes causadores destes problemas pode-se citar a mineração e agricultura predatórias, o comércio ilegal de madeiras, o florestamento mal projetado e o crescimento urbano desordenado (VELDMANN et al., 2015; DURIGAN; RATTER, 2015; FERNANDES et al., 2016; CARVALHO et al., 2019).

No Brasil, esses problemas têm se pronunciado nos últimos anos, em particular a partir de 2006, quando produtores de soja e carne voluntariamente comprometeram-se informalmente junto ao governo brasileiro a não mais desmatar a floresta amazônica para a produção de suas commodities, envolvendo nesse acordo, inclusive, os demais entes das respectivas cadeias produtivas (GIBBS, 2015). Conhecido como “Moratória da Soja e da Carne”, este acordo tinha por meta diminuir o desmatamento e destruição da floresta amazônica e de fato conseguiu atingir estes objetivos enquanto durou, porém, acabou por deslocar as pressões antrópicas para as savanas brasileiras, principalmente para o Cerrado. Assim, enquanto as áreas degradadas de floresta amazônica lentamente se recuperavam, novas áreas degradadas eram geradas no Cerrado brasileiro, a taxas muito maiores do que as de recuperação de floresta. Como resultado, as áreas de savana

passaram a comportar mais da metade das fazendas brasileiras, sendo sua maioria no Cerrado (SOUZA et al., 2020).

Com o tempo, a moratória foi sendo lentamente subvertida, adiada ou mesmo abandonada, de tal modo que, atualmente não é mais observada por nenhum dos agentes inicialmente envolvidos. O atual cenário político brasileiro tem resultado não só no retorno das pressões exploratórias e irracionais sobre a amazônia brasileira, mas também seu incremento em níveis que ameaçam a resiliência da floresta, incluso aí seus componentes savânicos (BARBOSA; FEARNSIDE, 2005a,b; BARNI et al., 2015; ALIX-GARCIA; GIBBS, 2017; FLORES et al., 2021; GOMES et al., 2020). Atualmente, este incremento está diretamente ligado às políticas de extrema direita do governo Bolsonaro, que tem atendido acriticamente todas as demandas de ruralistas, garimpeiros, madeireiros e mineradores. Também tem enfraquecido os instrumentos governamentais de gestão, monitoramento e fiscalização ambientais. Esse enfraquecimento se dá quer através de discursos e posicionamentos oficiais aberta ou veladamente desfavoráveis à questão ambiental, quer através do controle destes instrumentos por militares de alta patente que não têm a formação técnico-científico necessária para lidar com as questões ambientais (CARVALHO et al., 2019; FERRANTE; FEARNSIDE, 2019; SCHMIDT; ELLOY, 2020).

As savanas amazônicas estão profundamente ameaçadas pela expansão da fronteira agrícola, minerária e urbana para dentro de seus domínios. Um importante vetor de transformação e destruição das savanas amazônicas tem sido a abertura de estradas tanto para fins de melhoria da infraestrutura urbana e rural, como para escoamento da produção. Independentemente das estradas em questão, elas atuam como cabeça de ponte para a expansão da colonização humana e/ou das suas atividades exploratórias, resultando em mais desflorestamento e pressão por recursos naturais (BARNI et al., 2009; BARBER et al., 2014; FEARNSIDE, 2015). Quando associadas à exploração agrícola e/ou mineral, essas pressões tornam-se ainda maiores e podem degradar irreversivelmente alguns ecossistemas, comunidades ou populações amazônicas, incluindo aquelas das comunidades originárias (BANERJEE et al., 2021).

Em se tratando de savanas amazônicas, as consequências de incêndios antrópicos podem ser até mesmo catastróficas se eles queimarem toda a área de uma ecorregião (ALVES; PÉREZ-CABELLO, 2017). O manejo com fogo está ligado

à maioria das práticas agrícolas observadas na savana, uma vez que ele é empregado tanto para limpar o material derrubado, quanto para limpar os resíduos de colheitas. Em ambos os casos, é bastante grande o risco de o fogo escapar para além das fronteiras agrícolas e causar danos às formações mais sensíveis (como matas ripárias e buritizais). Antigamente, incêndios naturais na região amazônica eram mais numerosos do que incêndios antrópicos, porém, ultimamente estes últimos ultrapassaram em muito o número de incêndios naturais (DONG et al., 2021; KELLEY et al., 2021).

Roraima tem enfrentado um significativo aumento da exploração em seu território, seja devido à sua natureza pródiga quanto à existência de recursos naturais de interesse econômico (biológicos, geológicos e humanos), seja devido ao aumento populacional expressivo que o estado vem experimentando – principalmente devido à imigração venezuelana, que responde atualmente por praticamente um quinto da população (FURLEY, 1994; VERAS, 2009; VERAS et al., 2012; DINIZ; LACERDA, 2014; ARAÚJO Jr.; TAVARES Jr., 2017). Em um estudo de 2011, identificou-se 1.986 km² de áreas antropogenicamente perturbadas nas savanas de Roraima, dos quais 82,2% nas áreas de vegetação aberta (savanas típicas) e 17,8% em seus ecossistemas florestais associados, sendo a abertura de estradas o principal vetor de destruição (BARBOSA et al., 2007; BARBOSA; CAMPOS, 2011). Até o presente momento, as principais formas de destruição da savana estão associadas à expansão da infraestrutura urbana e rural e, mais importante, à expansão da fronteira agrícola pelo agronegócio, que já utiliza mais de 22% das áreas de savana para a produção de commodities de alto valor agregado e alta demanda internacional, como soja, milho, algodão, madeira e carne (DINIZ; LACERDA, 2018; LIMA, 2020; MAPBIOMAS, 2022).

Como membro signatário da Convenção sobre a Diversidade Biológica (internacional) e tendo a ratificado, o Brasil está comprometido a cumprir uma série de ações e protocolos dedicados a promover o desenvolvimento sustentável, o que inclui a criação e implementação de um plano nacional para alcançar estes objetivos. Conhecido pelo acrônimo “EPANB” (Estratégia e Plano de Ação Nacionais para a Biodiversidade), o plano brasileiro tem cinco objetivos estratégicos com várias metas cada um, dentre as quais estão a redução das perdas de habitats nativos e a recuperação de ecossistemas que proporcionam serviços essenciais (BRASIL, 2022). A exemplo das demais savanas do país, o Lavrado proporciona também

inúmeros serviços essenciais, como, por exemplo, conter grande diversidade de espécies de fauna e flora, muitas das quais endêmicas (BARBOSA et al., 2007), ser o local de recarga de águas subterrâneas do Sistema Aquífero Boa Vista, responsável por 70% do abastecimento público do estado (WANKLER; SANDER; EVANGELISTA, 2012), ser o local de vida e desenvolvimento de comunidades originárias e ser o local de lazer e turismo da população roraimense (BARBOSA et al., 2007). O cumprimento das metas do EPANB passa pelo entendimento da estrutura e dinâmica dos meios biótico, físico e antrópico do Lavrado, o que está ainda sendo construído.

Frente ao exposto, urge a necessidade de estudos que visem ajudar a compreender e descrever as características da savana roraimense, bem como dos processos geológicos, geomorfológicos, pedológicos, hidrológicos e ecológicos que atuam na criação e manutenção da biodiversidade savânica, com destaque à dinâmica de interação entre o meio biótico e abiótico. Embora existam muitos trabalhos sobre a savana de Roraima, muito ainda resta por saber sobre esse frágil ecossistema. Seu uso sustentável passa pelo entendimento das características, relações e histórico envolvidos, sem o qual toda e qualquer tentativa de preservação pode ser em vão. Entender a savana roraimense é importante também para garantir a segurança hídrica e alimentar de muitos municípios do estado, uma vez que é nela em que os principais cultivos agrícolas de larga escala são feitos e em particular, da capital Boa Vista, cuja principal fonte de água vem do Sistema Aquífero Boa Vista.

Neste contexto, a presente dissertação tem por objetivo quantificar os efeitos diretos e indiretos de alguns determinantes abióticos na variação espaço-temporal do Índice de Vegetação por Diferença Normalizada (NDVI), em um recorte da savana de Roraima, Brasil, englobando a Bacia Sedimentar do Tacutu. Os controles com um suposto efeito indireto são as Rochas, as Formas de Relevo, a Altitude e a Declividade. Controles com suposto efeito direto são: Temperatura, Precipitação, Frequência de Inundação, parâmetros dos solos relacionados à fertilidade Capacidade de Troca Catiônica (CEC) e Estoque de Carbono Orgânico (SOCS) e os parâmetros dos solos relacionados à textura Densidade Aparente e Percentagem de Areia. As principais hipóteses são o efeito positivo da precipitação, CEC, SOCS e percentual de areia, e o efeito negativo da inundação e da densidade aparente. Além disso, é provável que rochas e formas de relevo controlem indiretamente o NDVI,

uma vez que a distribuição da vegetação tem sido relacionada à dinâmica sedimentar quaternária em outros locais da Amazônia.

2 ABIOTIC DRIVERS IN AN AMAZON SAVANNA USING MULTISENSOR REMOTE SENSING

Bruna Mendel

Stélio Soares Tavares Júnior

Pedro Aurélio Costa Lima Pequeno

PRONAT UFRR

brunamendeln@gmail.com

9 ABSTRACT

10 Savannas support great biodiversity and high levels of species endemism, occurring
11 worldwide, including in the midst of the dense Amazon rainforest, where they play an
12 important role as recharge areas for the Amazon watershed, which, given its
13 continental dimensions, plays a central role in the hydrological cycle. Despite their
14 importance, the ecological health of these ecosystems is threatened by the expansion
15 of agribusiness and the advance of global warming. The parameters that control the
16 large-scale distribution of savannas in the Amazon are still poorly understood. This
17 paper presents the verification and quantification of direct and indirect controls of
18 abiotic variables on the photosynthetic activity of the vegetation, represented by the
19 Normalized Difference Vegetation Index (NDVI) in a time series of 5 years, in a clipping
20 that includes the Tacutu Sedimentary Basin in Brazil, whose origin and deposition is
21 associated with the evolution of the Guiana Savannas. The abiotic variables used were
22 lithologies (rocks), landforms, altitude, slope, climate (precipitation and temperature),
23 inundation frequency, and soil parameters: Cation Exchange Capacity (CEC), Soil
24 Organic Carbon Stock (SOCS), bulk density, and sand percentage. A confirmatory
25 Structural Equation Modeling (SEM) analysis was applied to investigate hypothesized

26 causal relationships in a path diagram. Nine Sentinel-2 multispectral images from 2017
27 to 2021, ALOS PALSAR radar images and NASADEM digital elevation model were
28 used to construct the Flood Frequency and relief shape of the river plains by means of
29 Linear Spectral Unmixing (LSU) and fusion of optical and Synthetic Aperture Radar
30 (SAR) images in open source software. The results showed that NDVI varied 60%
31 between dry and wet periods. The current configuration of the landscape, expressed
32 predominantly by the Sedimentary Formation Boa Vista and the products of its
33 reworking, arranged in long planing surfaces, resulting from successive cycles of
34 erosion and deposition, punctuated by residual reliefs (inselbergs) indirectly affect the
35 NDVI, that is, rocks and relief forms affect the soils, which affect the NDVI. The
36 variables with direct effect explained 48% of the variation in NDVI, with bulk density
37 having the largest effect due to the presence of cohesive horizons that hinder root
38 establishment and water drainage in soils. The fertility indicators (CEC and SOCS) had
39 a negative effect because the soils are acidic and with high exchangeable aluminum
40 content. The effect of precipitation is positive, and the effect of flood frequency is
41 negative, and these hydroedaphic constraints are also evidenced by the positive effect
42 of sand concentration in the soils. This approach demonstrated the relevance of
43 landscape evolution, soil, and climate on the spatial and temporal distribution of
44 vegetation cover.

45 **Keywords:** Tacutu Sedimentary Basin, SAR, LSU, SEM.

46

47

48

49 **1. INTRODUCTION**

50 Natural grassland vegetation is a common feature of the world, occurring from
51 tropical climatic belt to temperate regions. Covering approximately 33 million km²,
52 savannas are a biome with xerophytic nature that is characterized by a mosaic of grass
53 and forest ecological formations (Fernandes et al., 2016), with a predominance of C4
54 herbs and species tolerant to fire and light (Ratnam et al., 2011). In the Amazon,
55 savannas occur within the Amazon Rainforest, generally as small discontinuous areas,
56 like those of Suriname, French Guyana, and the Brazilian states of Amapá, and Pará,
57 but also as a single, and large continuous area (68.145 km²) on the triple border
58 between Brazil, Guyana, and Venezuela. Of this triple frontier area, 62% is in Brazil,
59 particularly in the Roraima state, where this ecoregion is known as “Lavrado” (Barbosa
60 and Campos, 2011; Barbosa and Miranda, 2005; Barbosa et al., 2005; 2007).

61 Savannas are historically linked to regional climatic dry seasons and
62 occurrences of natural and human-induced fire (Pivello, 2011; Walker, 1987). These
63 conditions have selected tree species of cork bark, herbaceous species with dense
64 and hairy sheaths buds, and species with physical and chemical deterrents to avoid
65 herbivory (Mistry and Beradi, 2000). The occurrence of savannas is determined by
66 complex interactions involving species functional characteristics, species coexistence,
67 competition and facilitation, herbivory pressure, climate, resource availability, fire
68 regimes (Hoffmann et al., 2012; Lehmann et al., 2011; Oliveras and Malhi, 2016), soil
69 nutrients (Lloyd et al., 2008), cation exchange capacity and the balance between
70 evaporation, and soil water storage (Veenendaal et al., 2015). Until now, remains
71 unknown the exact relationships between these drivers, the order of importance of
72 each variable, how growth rates occur across environmental gradients, and how the

73 savanna transitions to another vegetation type (Archibald et al., 2020; Lehmann et al.,
74 2014).

75 On a global scale not only the determinants of the occurrence of savannas vary,
76 but also their magnitudes. Lehmann et al. (2014) believe that evolutionary history and
77 regional environmental differences are the likely drivers of functional relationships
78 between woody vegetation, fire, and climate across continents. In Amazonia, this
79 evolutionary and biogeographic history of the biotic and abiotic drivers of savanna
80 becomes even more evident when one considers its geological and geomorphological
81 development through time, where the drivers are inextricably linked together through
82 a sequence of ecological and evolutionary feedbacks whose history goes back at least
83 to the Miocene, with emphasis on the Quaternary (Higgins et al. 2011; Rossetti et al.
84 2019a, b).

85 Savannas are largely ignored in the world's sustainable development agendas,
86 despite being under serious threat from ongoing degradation, mainly by the expansion
87 of agribusiness, urbanization, exploitation for natural resources and the rising of the
88 atmospheric CO₂ due the climate change (Bardgett et al., 2021; Lehmann and Parr,
89 2016; Pennington et al., 2006; 2018). In Brazil, half of the arable land is in their
90 savannas, and because of that, it is one of most threatened ecosystems of the country
91 (Souza et al., 2020). In Roraima, the savannas have faced great anthropogenic
92 pressure not only the urban and rural family farming development and urban
93 expansion, but mainly for extensive agribusiness exploration which has already used
94 22% of the savanna areas for the to road construction, planting of soy, maize, cotton
95 and meat, commodities of high added value and international demand (Araújo Jr. and
96 Tavares Jr., 2017; Barbosa and Campos, 2011; Diniz and Lacerda, 2018; Lima, 2020;
97 MapBiomas, 2022; Veras et al., 2012).

98 Due to their great biodiversity and their high levels of species endemism, as well
99 as their fundamental role as aquifer recharge zones, the importance of the world's
100 tropical savannas has been increasingly recognized (Carvalho and Mustin, 2017;
101 Furlan et al., 2020; Miller et al., 2012; Villalobos-Vega et al., 2014; Wankler et al.,
102 2012). Understanding how savannas shape themselves under different environmental
103 constraints and in landscapes with different evolutionary histories has provided
104 important insights into the distribution of species, especially in transition areas with
105 forests, which are particularly sensitive to environmental changes (Murphy and
106 Bowman, 2012). In this context, where the functioning of savanna ecosystems is
107 deeply threatened by climate change (Matías et al., 2021; Ramos et al., 2021), efforts
108 to quantify the drivers have been made at different scales, and for large areas, open
109 databases and remote sensing are indispensable tools (Hill Sources, 2021).

110 Thus, although the savanna of Roraima has similarities with savannas
111 elsewhere in the world and in Brazil, it is important to study its specific local and
112 regional abiotic controls because its evolutionary history and elements is unique. To
113 quantify the influence of abiotic determinants of the greenness in an Amazon savanna,
114 this paper shows a qualy-quantitative methodology of measurement and comparison
115 of some abiotic variables in the spatio-temporal variation of the Normalized Difference
116 Vegetation Index (NDVI) in the region of Tacutu sedimentary basin (Roraima, Brazil).
117 The variables with indirect effect analyzed were Rocks, Landforms, Altitude, and Slope,
118 and the predictors with direct effect were Temperature, Precipitation, Flooding
119 Frequency, and the soils parameters: Soil Cation Exchange Capacity (CEC), Soil
120 Organic Carbon Stock (SOCS), Soil Bulk Density (Density) and Soil Sand Percentage.

121 The main hypotheses related to the analysis are: (1) There is a high variation of
122 NDVI throughout the year (Xaud et al., 2009); (2) Geology and geomorphology affect

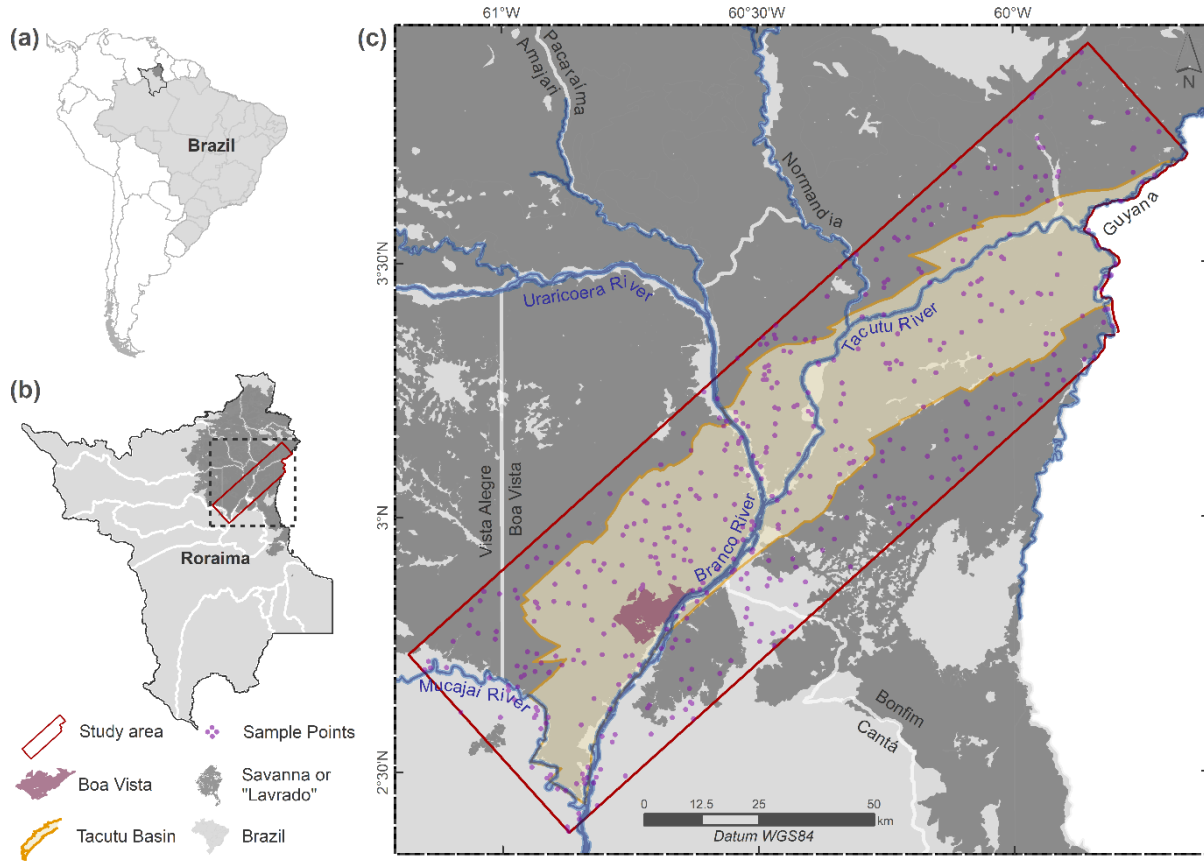
123 indirectly the NDVI, since vegetation has been related to recent sedimentary deposition
124 elsewhere in the Amazon (Cordeiro et al., 2016; Higgins et al. 2011; Rossetti et al.
125 2019a, b); (3) Although savannas in South America are not as affected by rainfall in
126 the same way as in Africa and Australia are (Lehmann et al. 2014), a strong effect of
127 precipitation is expected to be found here, as rainfall is voluminous and concentrated
128 in a few months, followed by long dry periods (Barbosa et al., 1997); (4) Flooded areas
129 exert a limiting effect on NDVI (negative relationship) (Tao et al., 2016; Oliveira et al.,
130 2019) and (5) There is a high positive relationship between the soil fertility and NDVI
131 (Lloyd et al., 2008; 2009).

132

133 **2. MATERIAL AND METHODS**

134 **2.1. LOCATION AND SAMPLING**

135 With 9,676 km², the study area is located along a SW-NE axis that extends from
136 the capital Boa Vista to the city of Bonfim, Roraima state, Northern Amazonia. The
137 study area was delimited by the extrapolation of the Brazilian portion of the Tacutu
138 sedimentary basin, that extends to Guyana, according to the limits proposed by Hahn
139 et al. (2012), being the limits of the first represented by a red polygon and the basin
140 area represented by an orange filled polygon (Fig. 1). The present work proposes to
141 measure the direct and indirect effects of abiotic variables in the vegetation vigor
142 variation in this predominantly savanna region. The studied area included less than
143 10% of forest, but their effects on the analyses conducted here can be neglected, since
144 the savanna-forest limits are not necessarily abrupt (many times they take place
145 gradually), and there are many patches of forested savannas or even non-savannic
146 forest inside the savanna area itself (IBGE, 2012; Meneses and Costa, 2012; Silva et
147 al., 2022).



148

Fig. 1. Location Map: (a) Brazil, South America, (b) Roraima state and (c) Study area (red polygon) in the savannas (BDIA, 2021) of the Brazilian portion of the Tacutu Sedimentary Basin (Hahn et al., 2012), with emphasis on sample points indicated by the purple dots.

149 The analyzes conducted here were based on data extracted from 500 points
 150 randomly distributed in the studied area (Fig. 1), in a way that at least 25% of the points
 151 were representative of the floodplain and frequently flooded areas. To include the
 152 climatic seasonality through time, a historical series of nine dates between 2017 and
 153 2021 were used, and in each one the same 500 points were used for extracted the
 154 data, totalizing 4.500 sampling units. For each one of the sample points, 18 variables
 155 were extracted, one NDVI biotic response variable, and 17 abiotic variables:
 156 precipitation lag times (4), temperature lag times (4), flood frequency (1), altitude (1),
 157 slope (1), geomorphology (1), geology (1), and soils parameters (4). The four lag times
 158 correspond to one to four months of accumulated precipitation and average

159 temperature. The four soil parameters used were: soil bulk density, cation exchange
160 capacity, sand, and soil organic carbon stock. Thus, the NDVI, flood frequency,
161 precipitation, and temperature were time and space variables, while all other variables
162 varied only in space. The extraction methods of each one of these variables will be
163 described separately in the following topics.

164

165 **2.2. SAVANNA VEGETATION**

166 Two great savanna vegetation groups are recognized in Amazon Biome, the
167 savanna itself and the steppe savanna, both with grassland, parkland, open woodland
168 and woodland subgroups which may or may not present a gallery of palms along
169 streams (Barbosa et al., 2007; IBGE, 2012). Miranda and Absy (2000) observed that
170 the distinction between these two great groups is more geographical than
171 phytosociological and they not described steppe savanna in Roraima.

172 In the area studied here, only the parkland and the grassland are recognized
173 (Barbosa et al., 2007). The parkland savanna shows a physiognomy characterized by
174 patches of woody elements and the grassland savanna is characterized by a
175 predominant grassy stratus where may have wood and wood shrub species of small
176 size in some cases. Besides, there are another vegetation formations too, as forest
177 islands (usually circular), gallery forests at river and streams ("igarapés") and palm
178 swamps of *Mauritia flexuosa* ("Buriti") along small seasonal streams (Barbosa and
179 Miranda, 2005; Santos et al., 2013). The extrapolated study area ended up
180 encompassing some tropical seasonal rain forests too (<10%).

181 For the analysis proposed here, the vegetation was represented by an index,
182 and the savanna was treated as a unity, that is, no distinctions were made between
183 their internal subgroups, mainly because there is not a good spatial resolution in the

184 maps available and doing such mapping job is beyond the scope of this paper. By the
185 same reasons, no distinctions were made between the woody and grassy elements of
186 the savanna.

187 The Normalized Difference Vegetation Index (NDVI) was applied to the high
188 spatial, spectral, and temporal resolutions Sentinel-2A images, acquired by
189 multispectral instruments of identical satellites that operate in the same orbit and that
190 went launched by the European Space Agency (ESA) on June 23, 2015 (Sentinel-2A)
191 and on March 7, 2017 (Sentinel-2B). The images captured by the Sentinel-2 sensors
192 have significantly contributed to the advance of the global vegetation knowledge,
193 including pointing seasonal differences in savannas (ESA, 2018; Macintyre et al.,
194 2020; Misra et al., 2020).

195 Whole images with low cloud interference were selected in each one of the four
196 tiles needed to cover the area, namely the T20NQJ, T20NQH, T20NRK and T20NRJ
197 from 2015 to 2021 temporal series. Although the satellites revisit interval is a few days,
198 only nine dates fulfillment the low cloud cover condition for the complete mosaic of the
199 area, an expected result to tropical regions, especially in the Roraima savanna, where
200 the rainy season shows a bigger cloud dominance than the Central and South Amazon
201 (Petri et al., 2019). Previous historical series studies in Roraima savanna showed that
202 the higher and the lower NDVI values were closely related to wet and dry periods
203 respectively (Gurgel et al., 2003; Xaud et al., 2009). The 32% variation in the NDVI of
204 this phenoregion is the third highest already recorded in the whole Amazon region
205 (Silva et al., 2013).

206 The nine Sentinel-2 images Level 1C used were: 02/15/2017, 02/20/2018,
207 09/18/2018, 10/08/2018, 04/01/2019, 09/13/2019, 03/26/2020, and 03/21/2021. The
208 images were converted to surface reflectance (BOA) Level 2A through the SNAP 8.0

209 Sen2Cor plugin, an open platform developed by ESA for Sentinel products
210 applications. The red and infra-red bands of Sentinel-2 are the B8 and B4 bands, with
211 10 m of spatial resolution and wavelength centered on 842 and 665 nm respectively.
212 So, the NDVI calculus was realized according to the following equation: $N D V I =$
213 $B 8 - B 4 / B 8 + B 4$. Their product can be interpreted as the vegetation vigor measure or
214 cover density, where values close to +1 correspond to dense and greenish vegetation
215 covering.

216

217 **2.3. DIGITAL ELEVATION MODEL**

218 A Digital Elevation Model (DEM) was used to determine the drainage systems,
219 altitude, and slope. To obtain a better DEM for the studied area comparisons were
220 made between the Panchromatic Instrument ALOS AW3D30 DEM (Tadono et al.,
221 2014) and the v.3 interferometric radar of Shuttle Radar Topography Mission (SRTM)
222 DEM (Farr et al., 2007), and their derivations DEM ALOS PALSAR (PALSAR, 2015)
223 and NASADEM (Crippen et al., 2016). This comparison was made by DEM subtraction
224 to identify inconsistencies in the differences between the models, and the possible
225 processing errors resulting from the application of global models to specific study
226 areas, as pointed out by Grohmann (2018).

227 The biggest inconsistencies were in the ALOS PALSAR DEM, that is the SRTM
228 pixels resampling from 30 to 12.5 m made originally to orthorectify the ALOS PALSAR
229 radar images, whose vertical accuracy has not been tested. The AW3D30, SRTM and
230 NASADEM models have similar vertical accuracy (proximately 5, 7, and 5.3
231 respectively), and AW3D30 seems to perform better in low relief areas, but in the area
232 studied here, it shows some noises, as their optical sensor was probably affected by
233 the frequent presence of clouds over this region (Mudd, 2020).

234 The SRTM and NASADEM showed little differences, and the latter was chosen
235 because it is an improved DEM whose altimetric precision was reprocess and
236 validated. NASADEM was project for Universal Transverse Mercator plan coordinates
237 through cubic convolution interpolation (Mudd, 2020), and then it was used for
238 drainage extraction on TerraHidro, an open-source tool developed in the C++ language
239 for hydrologic modeling (Rosim et al., 2003; 2008).

240

241 **2.4. SURFACE WATERS**

242 The drainage system of the Roraima savanna region is composed of an intricate
243 network of rivers, streams (igarapés), grassy swamps, buritizais (buriti palm streams),
244 and lakes. The drainage system has a predominant dendritic pattern in the SW portion
245 of the area and a parallel to a rectangular pattern in the central and NE portion, showing
246 a clear tectonic influence, in the form of rivers and streams captured by the Mesozoic
247 fault system associated with the formation of the Tacutu Basin and which were
248 reactivated in the Pleistocene by the syneclide formation processes that gave rise to
249 the Cenozoic covers of the area (Holanda et al., 2014, Nascimento et al., 2014). In
250 addition to the predominant drainage patterns aforementioned, trellis, radial, and
251 annular patterns are also observed.

252 The main rivers in the study area are the Tacutu, Uraricoera and Branco. The
253 Tacutu river originates in the Uaçari Hills, Guyana, in the tropical forest region and goes
254 North to the savanna region. Close to Conceição do Maú (3°33' N, 59°52' W), it
255 receives the waters of the Maú River and curves to the Southwest. Approximately 60
256 km ahead (3°22' N, 60°19' W), it receives the waters of Surumu River and at 45 km
257 ahead (3°01' N, 60°29' W) it joins the Uraricoera River to form the Rio Branco River,

258 keeping the Southwesterly direction until reaching the Rio Negro River ($1^{\circ}23' S$, $61^{\circ}50' W$), far from the Tacutu Basin Southwestern limit ($2^{\circ}26' N$, $60^{\circ}50' W$).

260 The hydrological year of this drainage systems responds to seasonal climatic
261 periods, with approximately one month interval of basin lag time. The Rio Branco
262 discharge has high amplitude: in July (wet season), during the flooding period, the river
263 reaches $7,000 m^3 s^{-1}$ and in March (dry season), during the ebb period, reduces to
264 $1,000 m^3 s^{-1}$, and the limimetric quotas can oscillate up until 6 meters (Carvalho et al.,
265 2021; Sander et al., 2008; 2015a, b).

266 Groundwater resurgences are very common and numerous, and it results in
267 ponds or lakes. Most of these ponds are temporary, and the lakes are often perennial.
268 In the wet season, the ponds and even some lakes can connect each other, forming
269 an intricate network of small streams with shared springs. Most of these lakes are
270 shallow, typically up to 2.5 m deep and their margins and other shallow parts used
271 have aquatic sedges (Cyperaceae) while in the deepest parts can be found some
272 floating leaves water lilies (Nymphaeaceae). Most of the lakes show an elevated
273 central zone formed by the sedimentary substrate remobilization during the surge of
274 the waters (Meneses et al., 2007; Sander et al., 2012; 2015a, b).

275 The studied area contains different sedimentary facies reworked and still in
276 formation (Latrubesse and Nelson, 2001; Menezes and Wankler, 2020). From all
277 environmental and sedimentary facies of an alluvial plain (Miall, 2006; Charlton, 2007),
278 only the floodplains were discretized and used in the analyzes conducted in this work.
279 For the objectives proposed here, the floodplains refer to the whole area of the river
280 channel plus the area formed by alluvial deposits, whether or not flooded by the river
281 overflow, the floodplains do not include areas flooded by lake overflow (lacustrine

282 plains). On the other hand, Flooding Frequency rates were generated for all areas
283 without distinction between their geomorphology unities.

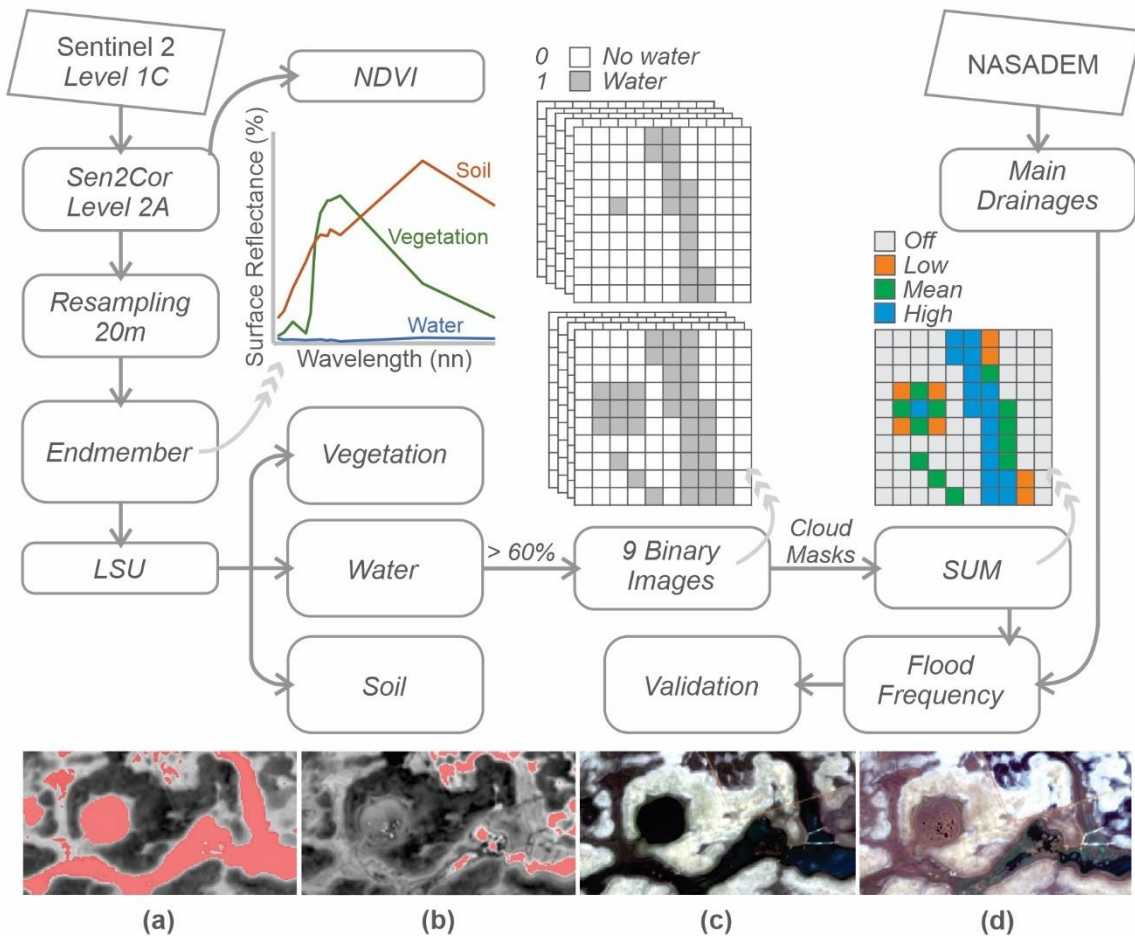
284

285 **2.5. FLOOD FREQUENCY**

286 Considering the nonexistence of systematic mapping of the recurrent flooding
287 areas, the Flood Frequency was mapped here. The same nine images of NDVI
288 analyzes were used, and 12 bands were considered: blue, green and red of the visible
289 spectrum, near-infrared with 10m of spatial resolution, the bands of the red edge, and
290 the short-wave infrared with 20m. Initially, the 1C Level images were converted to 2A
291 level images, next they were resampled from 10 m to 20 m to preserve the spectral
292 information (Fig. 2). The Linear Spectral Unmixing (LSU) model was applied, and to
293 their elucidating, it is necessary to consider that the instantaneous field of view
294 projected by the optical system of the sensor determines the size of the smallest object
295 that can be identified in an image since only objects with a size greater than the spatial
296 resolution are identified by definition. The satellite sensors record the interaction of
297 electromagnetic radiation with multiple components of the resolution elements of the
298 terrain, geometrically expressed by the pixel, whose values vary within a gray level
299 scale (2^n bits, where n is a function of the radiometric resolution) (Meneses and
300 Almeida, 2012). So, each pixel shows the reflectance integrated sum of all contained
301 objects, that is, the spectral responses of components are mixed in the pixel. If these
302 responses are known and considering the mixture as a linear combination, then it is
303 possible to estimate the proportion of the mixed objects (Holben and Shimabukuro,
304 1993; Shimabukuro and Ponzoni, 2017).

305 In each image endmembers were selected, that is, unmixed pixels containing
306 exclusively vegetation, water or soil from which the LSU tool Unmix 1.1 of SNAP 8.0

307 returned three abundance images with the probable proportion (0 to 100%) of these
308 components in each studied date. The 60% threshold was applied in the water
309 abundance image to discretize the water (Fig. 2a, b), and the resulting binary image
310 indicates the water absence (0) or presence (1). Sentinel-2's automatic cloud mask
311 has been applied. The binary images of the nine dates were sum (Zani and Rossetti,
312 2012). The main NASADEM extracted drainage was added to this sum, so a flooding
313 relative frequency gradient was obtained. For the product assessment, areas with high,
314 average, low or zero flood frequency were represented by 20 plotting points each,
315 totaling 80 points. These points were visually checked in the RGB color composition
316 images, and the information about the water presence (Fig. 2c) or absence (Fig.2d)
317 was tabulated, and their sum was compared to that of LSU product.



318

Fig. 2. Linear Spectral Unmixing flowchart applied to the determination of flood frequency. Water abundance in the wet (a) and dry (b) periods with 60% threshold for discriminating water (highlighted in pink). Example of the visual check performed for validation in wet (c) and dry (d) situations (notice the circular temporary lake).

319

320 2.6. FLOODPLAIN

321 Considering the importance of vegetation associated with floodplains, including
 322 those on smaller rivers (Drucker et al., 2008), these features were delineated here by
 323 merging optical and microwave images. Two images from different sensors were
 324 combined to form a new hybrid image via principal component analysis (Kulkarni and
 325 Rege, 2020; Mahyoub et al., 2019), with adaptations to the technique to highlight fluvial
 326 morphologies (D'Addabbo et al., 2016; Souza Filho and Paradella, 2005; Ward et al.,
 327 2014). SAR images can penetrate cloud cover and are independent of daylight

328 (Moreira et al., 2013; Shao et al., 2020), an alternative in the face of the difficulty in
329 obtaining satellite images of tropical forests where high precipitation rates and cloud
330 cover compromise optical multispectral images (Sanchez et al., 2020).

331 Alos Palsar and Sentinel-2A were employed as SAR and optical data,
332 respectively. The Advanced Land Observing Satellite (ALOS) Phased Array type L-
333 band Synthetic Aperture Radar (PALSAR) instrument operated in the L-band (1.27
334 GHz) producing day and night observations in a Japan Aerospace Exploration Agency
335 (JAXA) mission between 2006 and 2011 that are available on the Alaska Satellite
336 Facility platform (<https://ASF.alaska.edu/>). In this study, the PALSAR images used are
337 complex single look Level 1.1 data of Fine Beam Dual (FBD) imaging mode with HH
338 and HV polarization (horizontal transmission with horizontal reception and horizontal
339 transmission with vertical reception), 20m spatial resolution, acquired in 2009, date
340 and orbit: 03/07:18322, 15/07:18497, 20/07:18570, 01/08:18745 and 18/08:18993.
341 The pre-processing steps were performed in Sentinel Application Platform (SNAP) 8.0
342 software (Fig. 3a). Initially, deskewing was performed to bring the images to center
343 doppler zero, multilooking to adjust the pixel dimensions, Lee filter with 5 x 5 window
344 size to reduce speckle noise, Range-Doppler terrain correction with DEM ALOS
345 PALSAR, radiometric calibration to obtain the scattering coefficients in dB ($\sigma H H 0$ and
346 $\sigma H V 0$) and finally mosaicking and clipping of the study area. Sentinel-2A optical
347 imagery was acquired on March 1, 2020, Level 2A, already at Bottom Of Atmosphere
348 reflectance. SAR and optical images were registered in TerraView 5.5.2 software, with
349 Root Mean Square Error (RMSE) less than one pixel.

350 In TerraView 5.5.2 the Sentinel 2A images were mosaicked and cropped, then
351 PCA was applied to transform the multispectral images into new components with high
352 spectral variance (Fig. 3b). The PCA was performed for the visible (PCA-1: bands 2 to

353 4), shortwave infrared (PCA-2: bands 11 and 12) and near-infrared and red edge (PCA
354 3: bands 5 to 8A) band sets, the first component of each was used to generate an RGB
355 image, which was transformed to the IHS color space (intensity, hue and saturation)
356 and in the inverse transform the vector I was replaced by the Alos Palsar image, thus
357 resulting in the hybrid image. The hybrid image was segmented by region growth, the
358 segments were sorted by k-means, and finally, the floodplain polygons were manually
359 edited.

360

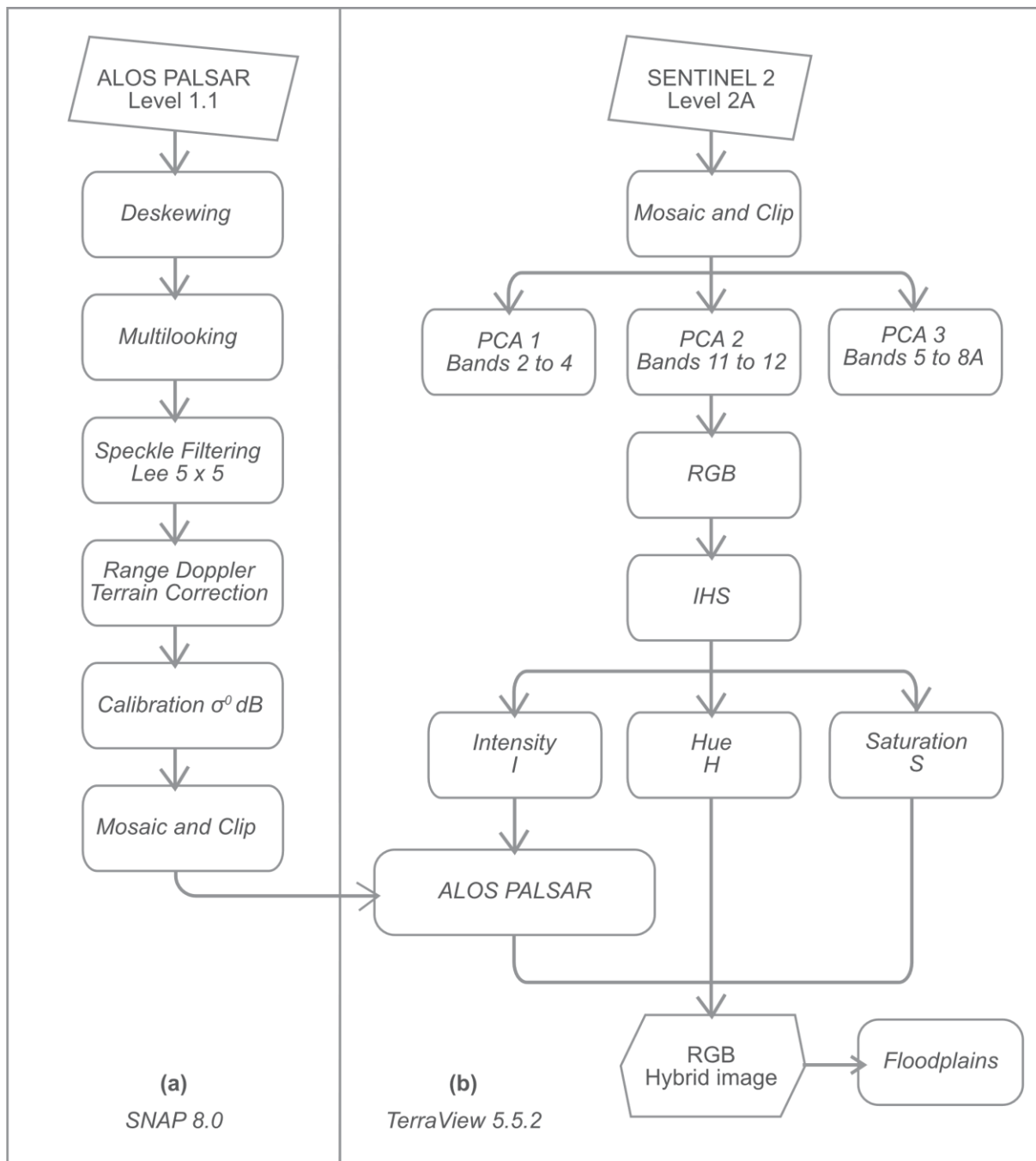


Fig. 3. Floodplains flowchart: (a) Preprocessing in SNAP 8.0. (b) Fusion in TerraView 5.5.2.

361

362

363 2.7. CLIMATE

364 According to Köppen-Geiger, the climatic type of the region is the Savannic –
 365 Aw, which is characterized by dry (October-March) and wet (April-September) periods
 366 well distinct, locally known respectively as “summer” and “winter”. Only 10% of the
 367 annual rains (~1500 mm) occur during the dry period, the remaining 90% are

368 concentrated in the wet period, being more than half during the May-July interval
369 (Barbosa, 1997). The climate is hot and humid, with an average temperature of 25 °C,
370 generally being January the driest month, with precipitations below 60 mm (Meneses
371 et al., 2007). The cyclic Pacific warming (El Niño) and cooling (La Niña), as well as the
372 global climate change caused by burning fossil fuels have affected the rainfall intensity
373 and the water regime, in Roraima this effect also intensifies the risks of flooding and
374 fire (Barni et al., 2022).

375 The climate data were obtained from the Global Land Data Assimilation System
376 (GLDAS) by National Aeronautics and Space Administration (NASA), which uses
377 advanced and robust modeling technics of assimilation and integration of remote and
378 terrestrial meteorological data to give consistent temporal products of the Earth
379 surface. The temporal resolution of the acquisition is three hour and daily, the months
380 subproducts are generate by the temporal mean of three hour data and made available
381 with 0,25° x 0,25° of spatial resolution, i.e., with a pixel of approximately 0.9 km
382 (Beaudoing and Rodell, 2020).

383 The temperature and precipitation data were organized to consider the climatic
384 annual and historical series, for which the dates used were the same those used to
385 NDVI and Flood Frequency. In a 26 years interval for the all Amazon region, Silva et
386 al. (2013) found the best correlations between precipitation and NDVI response in
387 precipitation lag-times of three months, but to the specific regions of savanna the better
388 responses occurred in lower lag-times. Thus, the accumulated precipitation for one,
389 two, three and four months of precipitation lag-times were used, as well as the mean
390 temperature (°C) for each one of these same lag-times.

391

392

393 **2.8. GEOLOGY AND GEOMORPHOLOGY**

394 The study area encompasses the entire Brazilian portion of the Tacutu
395 sedimentary basin. With up to 300 km in length in the NE-SW direction and 50 km in
396 width, the basin is in the central portion of the Guyana Shield being part of it in Brazil
397 (4,500 km²) and part of Guyana (7,000 km²) – where is called North Savannas Rift
398 Valley Basin (Silva and Porsani, 2006). Their origin is related to the rifting processes
399 associated with the Pangea breakup in the Juro-Cretaceous that in the Central Atlantic
400 region split the Northwest of the old Gondwana from the Southwest portion of the old
401 Laurasia (Zalán, 2004). The breakup of Pangea also initiated the Andean orogeny,
402 whose progressive uplift culminated in the reversal of the direction of vergence of the
403 Amazonian watershed during the Miocene (Albert et al., 2018; Cediel et al., 2003). It
404 is speculated that the Rio Branco then completely changed its drainage system, in
405 which the rivers ceased to flow from the Guiana Shield towards the Caribbean Sea, to
406 flow towards the Rio Negro and ultimately the Atlantic (Cremon et al., 2016).

407 During the initial Pangea breakup phase and establishment of the Tacutu Half-
408 graben, tholeiitic basalts and andesites extruded around 150 Mya and formed what
409 today is known Apoteri Formation (Eiras et al., 1990; Reis et al., 2006). This large
410 space of accommodation generated gave rise to what is now known as the
411 sedimentary Tacutu Basin, which from the base to the top was filled by the following
412 sedimentary sequences: Manari Formation, Pirara Fm, Tacutu Fm and Tucano Fm
413 (Vaz et al., 2007).

414 The Manari sits discordantly on the Apoteri, and it is constituted by fine
415 siliciclastic materials as siltstones, shales and locally calcisiltstone and dolomites
416 deposited in Thitonian lacustrine environments (Crawford et al., 1985; Eiras et al.,
417 1990). The Pirara sits discordantly, and it is constituted by evaporitic halite in the

418 central basin area and shales, siltstones and carbonates in the basin margins,
419 deposited in lacustrine and sabkha plains (Silva and Porsani, 2006). The Tacutu sits
420 discordantly, and it is constituted predominantly by siltstones, sometimes calciferous,
421 sometimes clayish, and secondarily by sandstones, carbonates or shales, deposited
422 in shallow lacustrine environments during the Berriasian-Barremian interval (Crawford
423 et al., 1984; Santos et al., 2016; Souza et al., 2010; Hammen and Burger, 1966). The
424 Tucano rest concordantly and it is constituted by sandstones with or without kaolinite
425 and sometimes intercalated siltstones deposited in fluvio-lacustrine environments
426 during the Barremian-Albian interval (Reis et al., 1994; Cruz et al., 2019). Although
427 the Tacutu formation outcrops along some portions of the Arraia and Tacutu rivers, only
428 the Apoteri and Tucano formations are detectable at the map scale used here to the
429 studied area, covering approximately 1.7 and 4.1% of the area, respectively (Holanda
430 et al., 2014).

431 Long after the end of the Tacutu Basin infill, neotectonic reactivation of the faults
432 during the Pleistocene gave rise to a shallow intracratonic basin (syneclyse) filled by
433 Boa Vista Formation in two stages, the lower succession being controlled by the
434 structures of the Tacutu sedimentary basin, and the upper succession effected by the
435 complete flattening of the relief from a low gradient alluvial plain (Menezes and
436 Wankler, 2020). So, the Boa Vista Formation rest discordantly on Tucano Formation
437 and are characterized by sandstones, laterite, sandy claystones and conglomerates
438 deposited in fluvial, lacustrine and aeolian environments (Milani and Thomaz Filho,
439 2000; Montalvão et al., 1975; Reis et al., 2001; Vaz et al., 2007). Sandstones of the
440 Quaternary Areias Brancas Formation and recent alluvial deposits can be found
441 respectively over some parts of the Boa Vista Formation and along the beds or terraces
442 river. The Areias Brancas Formation is believed to be the result of reworking Formation

443 Boa Vista during the Pleistocene-Holocene (Latrubesse and Nelson, 2001). The Boa
444 Vista and Areias Brancas Formations cover 71% of the study area, respectively
445 (Holanda et al., 2014).

446 Based on lithology, structural lineaments, and stream patterns the area was
447 included in the Rio Branco-Rio Negro Pediplane Morphostructural Domain by Franco
448 et al. (1975), and now two geomorphological units are recognized, the Boa Vista
449 Depression and the North Amazon Dissected Highlands (Holanda et al., 2014), whose
450 predominant features are landforms modeled by accumulation/aggradation,
451 punctuated by dissection/denudation areas (Nascimento et al., 2014).

452 The accumulation modeled landforms included fluvial plains and an extensive
453 planation surface, subdivided in Planation Surface and Erosional Planation Surface,
454 this latter occurring as slightly elevated areas and being a result of smooth incision by
455 the streams. These planation surface developed on Boa Vista and Areias Brancas
456 sedimentary formations, and they are generally marked by smooth and low elevations
457 ("tesos") that are frequently associated to laterization processes. These areas are
458 characterized by seasonal flooding, incipient drainage constituted by intermittent
459 streamlets with associated *M. flexuosa* swamps (Franco et al., 1975; IBGE, 2009;
460 Ladeira and Dantas, 2014).

461 The dissection modeled includes inselbergs resulting from the pediplanation
462 process, and the Serra do Tucano hills and mounds, of the North Amazon Dissected
463 Highlands. These remaining structural highs appear amidst the Planing Surfaces within
464 the Tacutu sedimentary basin limits, or even as proterozoic residual highlands,
465 configuring the basin shoulders (Costa and Falcão, 2011; Silva et al., 2010).

466 The geological and geomorphological maps were based on the Geodiversity of
467 the State of Roraima vector maps (at a scale 1:1.000.000), available free of charge by

468 the Brazilian Society of Geology (Holanda et al., 2014). Some adjustments were made
469 in these vectors based on bigger scales works (Menezes and Wankler, 2020;
470 Nascimento et al., 2014; Zular et al., 2019), and on the floodplain polygons obtained
471 here according to the methodology described in the topic “2.2.4.1, Floodplain”. The
472 geological units were synthesized as a variable called “Rocks”, and each one of its
473 units was used to order them on a scale according to their hypothetical growing
474 influence on NDVI.

475 Since the variable Rocks encompass both rocks itself and unconsolidated
476 sedimentary material from alluvial plain, the scale is more related to the genesis than
477 to the nature of each unit. Among the sedimentary group, the Areias Brancas shows
478 higher reworking taxes, thus, lower NDVI values than the Boa Vista formation, while
479 the Tucano formation probably presents highest values of the group due to its sheltered
480 position from the floods. Metamorphic group, in turn, are likely to have higher values
481 than those of the sedimentary group due their ability to transfer nutrients to the soil
482 from their primary and secondary minerals. Similarly, the igneous group usually
483 generates more fertile soils and is therefore more likely to have higher NDVI values,
484 especially associated with the clay soils of the volcanic rocks. Finally, higher expected
485 NDVI values are associated with alluvial deposits given the riparian vegetation. Thus,
486 the Rock variable was ordered like this: Areais Brancas Fm (1), Boa Vista Fm (2),
487 Tucano Fm (3), Metamorphics (4), Plutonics (5), Volcanis (6) and Alluvial deposits (7).

488 The geomorphological units were grouped in the “Landforms” variable. The
489 modeled residual relief units on morphostructures formed in distinct tectonic episodes
490 were not discretized because they are beyond the scope of this work, so the altitude
491 was used to establish an ascending order for each one of the “Landforms” units in the
492 following way: Floodplains (1), Planation Surface (2), Erosive Planation Surface (3),

493 Tucano Hills (4), Inselbergs (5), and Mountains (6). The 1 to 3 features represent
494 accumulation modeled areas and the 4 to 6 represent dissection modeled areas (IBGE,
495 2009; Nascimento et al., 2014). The altitude map was based on NASADEM. The
496 declivity % map was extracted from NASADEM, and the percentage classes used to
497 follow the EMBRAPA (1979) recommendations: 0 – 3% smooth; 3 to 8% smooth-way,
498 8 to 20% wavy, 20 to 45% strong-wavy, and >45% mountainous.

499

500 **2.9. PEDOLOGY**

501 The soils of Roraima have great pedological diversity, products of rock
502 weathering and erosion and cyclic deposition in different biological and climatic
503 conditions acting both in geological and current time scales. In general terms, the
504 predominant soils are acid, aluminum saturated, with low cation exchange capacity,
505 kaolinitic, with low base sum and saturation, i.e., dystrophic, organic matter and
506 organic carbon poor. Considering the World Reference Base (WRB) for soil taxonomy
507 of FAO (2015), the main soils under savanna can be classified as yellow Ferrasols and
508 Acrisols, Ferralic Arenosols, Concretionary Plinthosols and Gleysols. Due to the
509 practice of burning during dry periods, they all tend to have low natural fertility and a
510 marked loss of organic matter (Vale Júnior and Sousa, 2005; Vale Júnior et al., 2014).

511 The yellow Ferrasols and Acrisols are deep and have a cohesive subsurface
512 horizon and their origin is due to the weathering of the Boa Vista Formation. In the dry
513 season, this cohesive horizon is especially hardened, making it difficult for the plants
514 to establish roots, and in the wet season this previous hardening causes expressive
515 laminar erosion by the intense runoff despite the low slope of the region. Associated to
516 these soils occur the Ferralic Arenosols, which are quartz sands on plain to slightly
517 wavy reliefs, with clay content below 15% and whose origin is due to the Boa Vista

518 Formation erosional reworking both in hydromorphic and aeolian environments
519 (Latrubblesse and Nelson, 2001; Vale Júnior and Schaefer, 2010). The grassland
520 savanna is more expressive in these cohesive and sandy soils.

521 The red Ferrasols and Acrisols develop on positive residual reliefs of volcanic
522 rocks and their color results from the presence of hematite even so the goethite
523 (yellow) is the dominant iron oxide. Despite the general chemical characteristics
524 described previously, these red soils are slightly more fertile than the yellows because
525 they are less cohesive, more porous, and well drained, which allows better root
526 development and, thus, the ability to sustain forest patches and parkland to woodland
527 savannas (Vale Júnior and Sousa, 2005). The colluvium is commonly associated with
528 positive residual reliefs both of Apoteri Formation volcanic rocks and of Guyana Shield
529 metamorphic rocks.

530 The Concretionary Plinthosols developed from the weathering of the red
531 Ferrasols and Acrisols by the groundwater fluctuations along the time, whose wet and
532 dry cycles promoted the iron redox. If on the one hand the ferruginous concretions
533 present in those soil decrease their permeability and difficult the root development, on
534 the other they play an important role for occupying the landscape edges and giving
535 slope sustaining, protecting these areas against erosion. Despite of their stoniness,
536 Concretionary Plinthosols tend to hold parkland savannas (Benedetti et al. 2011;
537 Feitosa et al., 2016).

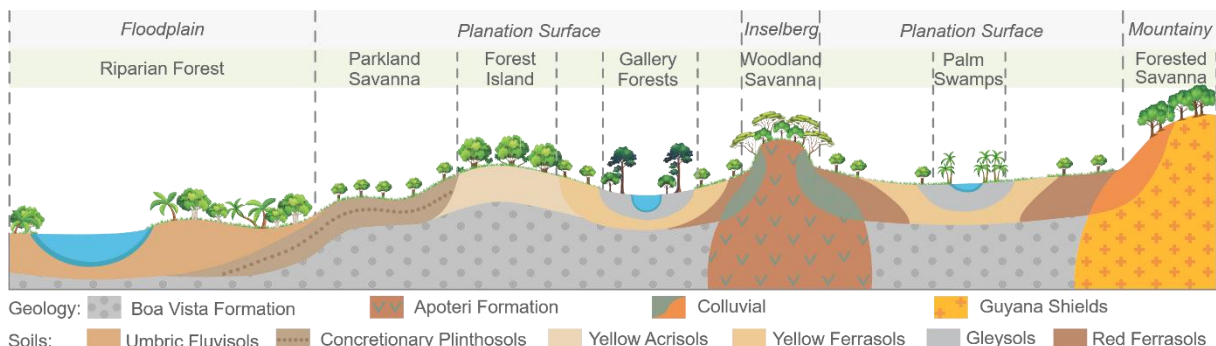
538 Gleysols are found on flooded areas, large and small streams, gallery forest and
539 palm swamps, and they are characterized by being deep, hydromorphic, and poorly
540 drained. Their typical grey color came from the reduction of the iron minerals by
541 stagnant waters. In fluvial plains there are also Umbric Fluvisols, characterized as
542 young soils in which the sedimentary input from rivers is accompanied by nutrients and

543 organic matter what gives to them the best fertility levels and the capacity to sustain a
544 lush riparian forest (Benedetti et al. 2011; Vale Júnior and Schaefer, 2010).

545 The soil variables were Cation Exchange Capacity (CEC), Soil Organic Carbon
546 Stock (SOCS), Soil Sand Percentage and Soil Bulk Density, all of them obtained from
547 SoilGrids, with 250 m of spatial resolution, whose interpolations were made with
548 satellite and field data (Hengl et al., 2017). The chemical CEC and SOCS variables
549 are related to the soil fertility and to the nutrient availability to vegetation; sand
550 percentage and bulk density are textural features and are related to soil drainage
551 (Zuquim et al., 2020), although soil texture is not a physiologically important edaphic
552 factor, it is correlated with other relevant environmental characteristics, such as nutrient
553 and water retention (Zuquim et al., 2014). All soil parameters were extracted from the
554 surface (<5 cm depth).

555 Fig. 4 synthesizes the study area characterization in a schematic section (out of
556 scale) and illustrates the main geological, geomorphological, pedological, hydrological
557 elements and the widely described and discussed savanna phytobiognomies
558 (Barbosa and Miranda, 2005; Barbosa et al., 2007; Benedetti et al., 2011; Carvalho et
559 al., 2021; Feitosa et al., 2016; Franco et al., 1975; Latrubesse and Nelson, 2001;
560 Menezes and Wankler, 2020; Reis et al., 2001; Vale Júnior and Sousa, 2005; Vale
561 Júnior and Schaefer, 2010; Xaud and Carvalho, 1999; Vaz et al., 2007). It should be
562 noted, however, that this scheme represents the units in their dominance occurrences
563 and relations, but they are not so linear and regular, since different soils bear the same
564 type of vegetational phytobiognomy, as well as there are distinct
565 phytobiognomies that can be found on a same type of soil, geological or
566 geomorphological unity.

567



568

Fig. 4. Schematic section of the study area with the main soils and their environments.

569

570 2.10. STRUCTURAL EQUATION MODELING (SEM)

571 The linear model used was the multiple linear regression model, which seeks to
 572 separate the possible direct effects among the predictors and isolate the independent
 573 effect of each on the variation of the independent/response variable. The model was
 574 built assuming the direct effect of predictors temperature, precipitation, flood frequency
 575 and soil parameters on NDVI, assumed ecological relationships follow those proposed
 576 by Guisan and Zimmermann (2000), rocks and relief are in an indirect effects model,
 577 as they affect soil parameters, which affect NDVI. Then, a confirmatory analysis of
 578 Structural Equation Modeling (SEM) was applied to investigate the hypothetical causal
 579 relationships between the variables in a path diagram, in which indirect effects are
 580 estimated by multiplying the coefficients along a given path in the diagram (Magnusson
 581 et al., 2015; Shipley, 2016). All statistical analyses were performed in R environment
 582 (R Core Team, 2013).

583

584 3. RESULTS AND DISCUSSIONS

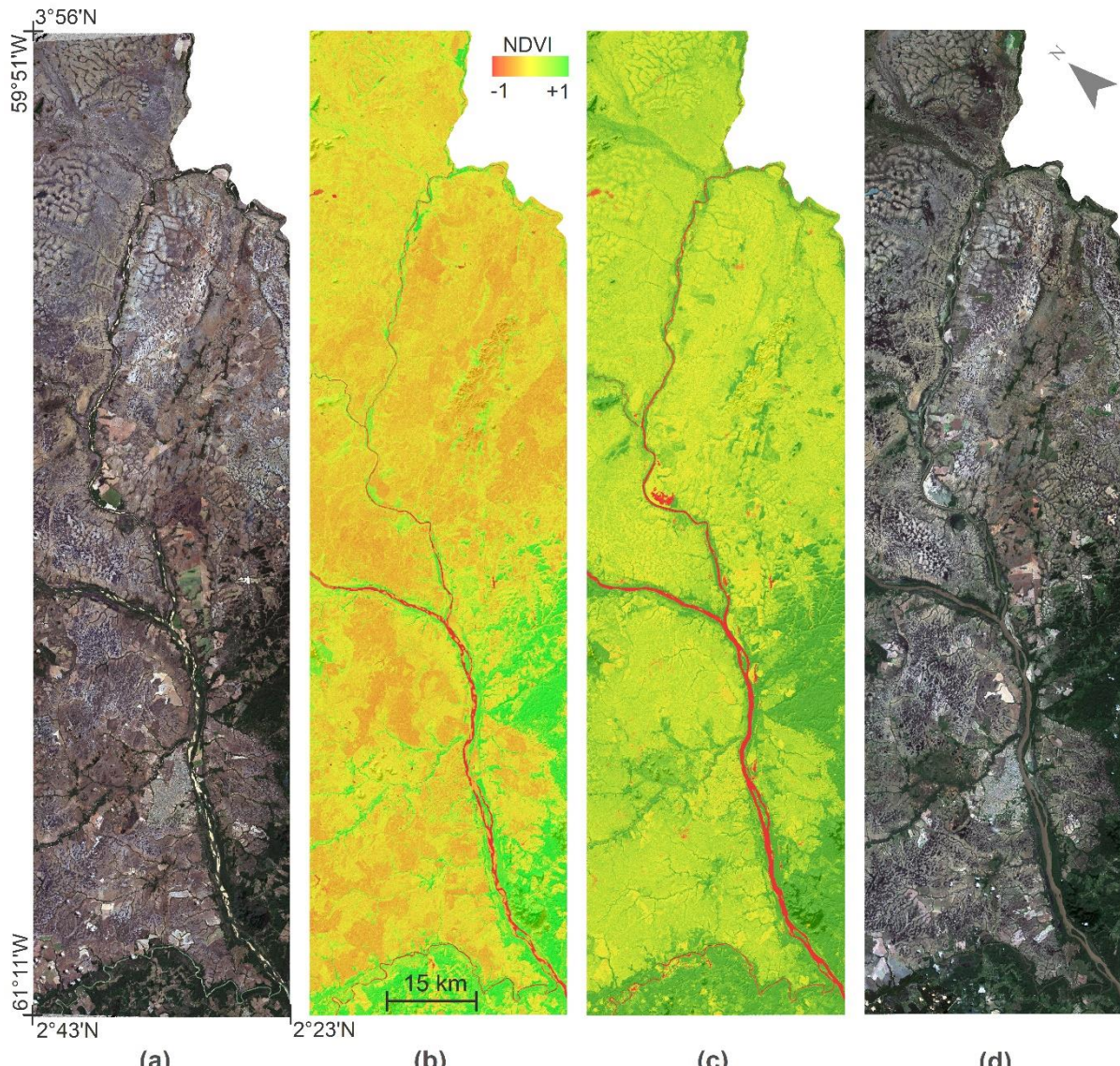
585 3.1. NDVI

586 The NDVI showed 60% variation on average between the nine analyzed dates.
 587 The lowest mean values occurred on March 26, 2020 (Fig. 5a, b) and were around

588 0.27 while the highest value occurred on September 18, 2018 and were around 0.48
589 (Fig. 5c, d). Besides this time variation, the NDVI also showed a wide spatial variation,
590 whose highest values (77%) were recorded on the same dates of high contrast
591 between vegetated and non-vegetated areas, i.e., on the same dates of lowest NDVI
592 values. The lowest spatial variations (46%) were recorded on the same dates as the
593 highest NDVI values – coinciding with the period in which the vegetation was more
594 homogeneous.

595 The photosynthetic activity and therefore the NDVI respond to climatic
596 seasonality (Silva and Klink, 2001), that is, the wetter the period, the higher the NDVI
597 and vice-versa. This occurs because the rain enhances in the soil the amount and
598 quality of resources needed for plants, such as humidity, nutrients and organic matter
599 (Ronquim, 2021). Although this relationship is positive along all savanna, it is controlled
600 by different vegetational strategies for each sub environment. Thus, the increase in
601 NDVI during the wet season occurs mainly in herbaceous plants due to the increase
602 in leaf area and the speed of vegetation reproduction, in woody species, the NDVI
603 responds to the increase in metabolism (Carrijo et al., 2021), common adaptation
604 strategies in savannas, also seen in grasses (Costa et al., 2011;2014) and trees and
605 shrubs (Ferreira et al., 2015) of Roraima's savannas.

606



607

Fig. 5. Sentinel 2A real color composition and corresponding NDVI. (a) Dry season image; (b) the lowest mean NDVI value on March 26, 2020; (c) the highest mean NDVI value on September 18, 2018, and (d) wet season image. The maps displayed in this section present the study area (Fig. 1) slightly rotated for better visualization of its different variables.

608

609 **3.2. FLOOD FREQUENCY**

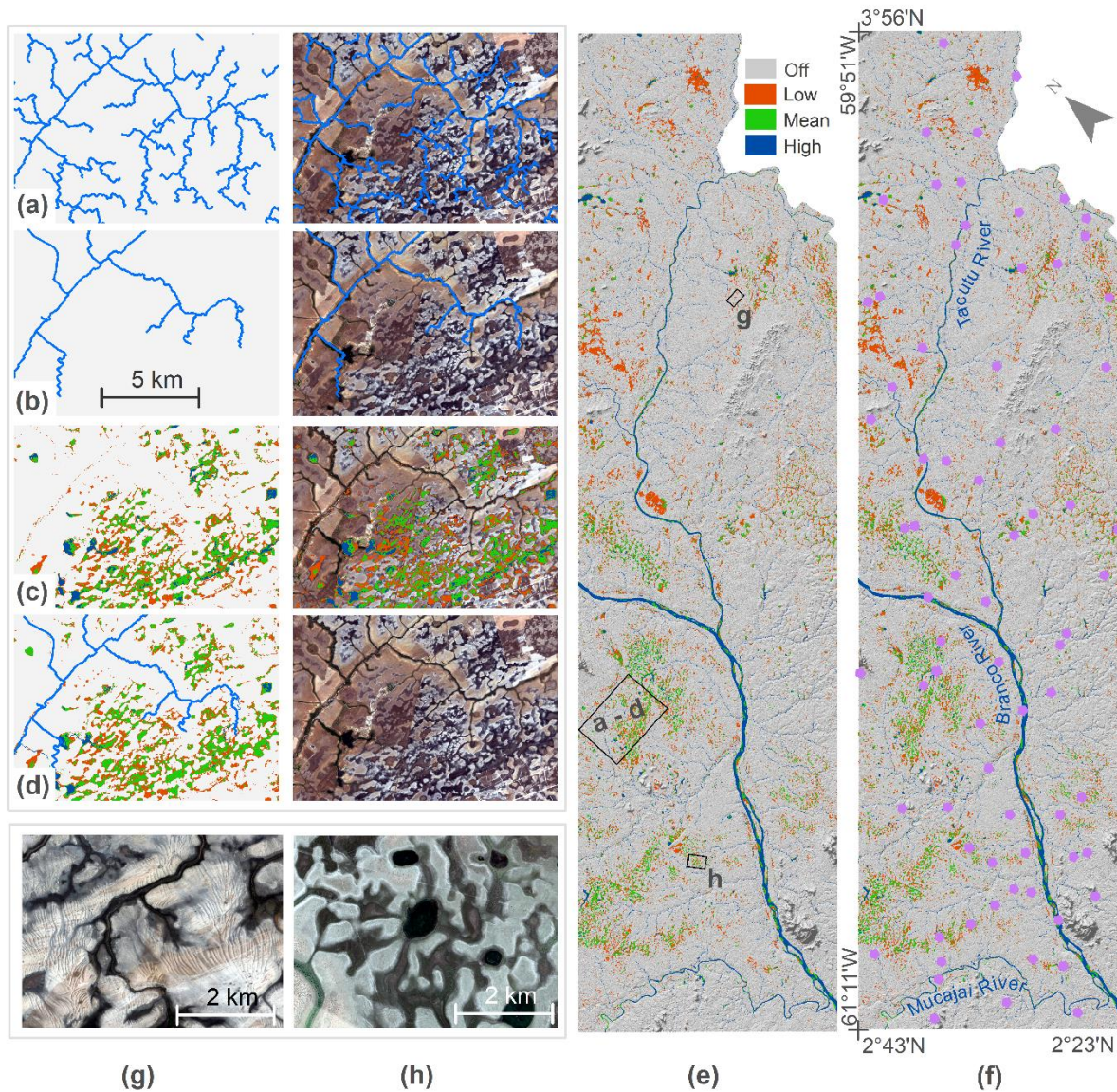
610 The automatic extraction of streams from DEM did not adequately represent
 611 the streams because the area is very flat and the NASADEM, although robust, does
 612 not have a detailed resolution to capture such small variations in slope. With a low
 613 threshold, the automatic extraction creates streams where they do not actually exist

614 (Fig. 6a) and with a high threshold only the main streams are revealed (Fig. 6b). On
615 the other hand, the LSU does not recognize the "igarapés" (small drainage) because
616 the riparian vegetation is dense in these locations throughout the year, regardless of
617 the season (Fig. 6c), so the main drainages extracted from the DEM were added to the
618 areas delimited by LSU to compose vectors that represent the complex drainage
619 system of the study area (Fig. 6d). The areas with low, medium and high flooding
620 frequency reached 472, 215 and 225 km² respectively, corresponding to 9.3% of the
621 total area analyzed and the mean NDVI of these areas was 0.25. The map in Fig. 6e
622 represents the "Flood Frequency", for the statistical analysis this predictor entered as
623 0 or 1, indicating absence or presence of flooding, since the 500 points (Fig. 1) were
624 extracted from each of the 9 images/dates in the time series.

625 The LSU fundamentally separates water or vegetation, and this is a technical
626 limitation to characterize the drainage system, as it makes impossible the discretization
627 of water bodies covered by vegetation, as is the case of some small streams and the
628 shorezone of lakes during the dry period (Meneses et al., 2007). These problems were
629 solved by the addition of the main small streams extracted from NASADEM and by the
630 lake identification through the temporal series. The validation of the LSU showed $r^2 =$
631 0.9 ($p < 0.001$) (Fig. 6f).

632 The flood frequency mapping made here highlighted the parallel river pattern in
633 the Tacutu River-Tucano Hills region and the dendritic river pattern in the Boa Vista
634 region (Fig. 6g and 6h), as proposed by Latrubesse e Nelson (2001). These differences
635 can be associated not only to the structural geology and geomorphology features but
636 with the climatic factors acting in both regions. The results obtained here also allowed
637 us to differentiate the two regions in terms of the scars left behind by the runoff, being
638 more biaxial opposite on the Tacutu River-Tucano Hills region and slightly radial in the

639 Boa Vista region. The higher and better precipitation distribution recorded to the
 640 Uraricoera and Mucajáí river catchments when compared to those recorded to the
 641 Tacutu river catchment explains why this latter lowers further in the dry season and
 642 contributes less to the Branco River than the two first (ANA, 2020).



643

Fig. 6. Drainages extracted from NASADEM with (a) low and (b) high threshold. (c) Flood areas delimited by the LSU. (d) Integration of b and c. (e) Flood frequency. (f) Distribution of points for LSU validation. Different surface runoff patterns associated with predominantly parallel (g) and dendritic (h) drainages.

644 **3.3. FLOODPLAIN**

645 The fusion of the Sentinel 2A multispectral image (Fig. 7a) with the ALOS
646 PALSAR SAR image (Fig. 7b) generated the hybrid image (Fig. 7c) from which it was
647 possible to extract the floodplains, and small streams (Fig. 7d), whose area of 1,305
648 km² constitutes 13.3% of the total area, allowing a better detailing in relation to the 484
649 km² obtained by the Brazilian Geological Survey made at 1:1,000,000 scale (Holanda
650 et al., 2014). The prominence of the floodplains was given by the double jump effect in
651 radar images, the signal return is enhanced by the flooded areas (Pierdicca, 2013).
652 The signal return is enhanced by flooded areas (Moreira et al., 2013) made manual
653 separation difficult, but since they occur in less than 10% of the total area, it only
654 required more attention during the process of dividing floodplains by forest. The area
655 of the river plain is larger (1,305 km²) than the flooded areas (912 km) because it also
656 considered the discrimination of alluvial deposits, which are not necessarily periodically
657 flooded.

658 The sediments of the Branco River floodplain are richer in illite and potassium
659 than those further away (Meneses et al., 2007), which favors the development of
660 vegetation. The smaller floodplains also have associated riparian vegetation. In fact,
661 NDVI in the studied area were on average higher in the floodplain (0.56) than outside
662 (0.32), coinciding with the higher concentration of tree vegetation in the savanna area.

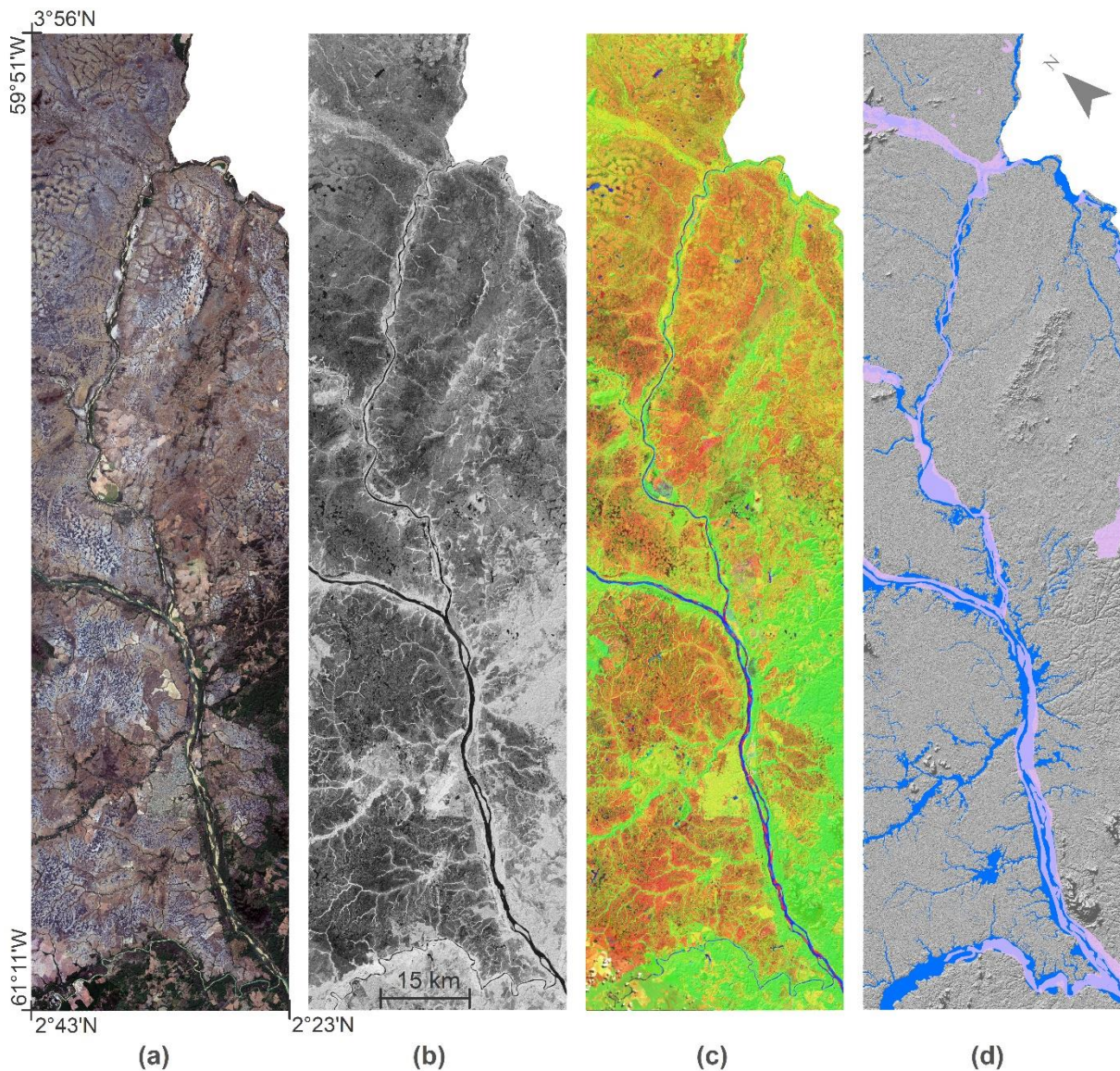


Fig. 7. (a) Sentinel 2A multispectral image. (b) ALOS PALSAR image. (c) Hybrid image. (d) Floodplain extracted from the hybrid image (blue), and floodplain overlay from the Brazilian Geological Society (pink).

664 3.4. TEMPERATURE AND PRECIPITATION

Ranging around 5%, the temperature did not fluctuate much, which is expected for the hot climate of the region – with average temperatures between 28°C and 32°C (Fig. 8a, b). In space, the temperature varied on average by 2%. Precipitation showed 95% variation over time, confirming the expected well-demarcated seasonality, so that the minimum accumulated rain was 14 mm on March 26, 2020, in the “summer” period, while the maximum was 222 mm on September 18, 2018, in the “winter” period (Fig.

671 8c, d). The precipitation variation in space was 30% on average, with a minimum of
672 20% on September 13, 2019 and a maximum of 53% on April 1, 2019. As the predictive
673 power of the different lag-times (30, 60, 90, and 120 days) was similar, 30 days were
674 used for the temperature and precipitation variables, since this is the interval commonly
675 observed between the maximum rain volume and curve pike in the hydrograph of these
676 rivers (ANA, 2020; Sander et al., 2015a, b).

677 Precipitation is one of the main drivers of savanna distribution (Lehmann et al.,
678 2014). In tropical savannas, the peak of vegetative growth coincides with the rainy
679 season because the temperature is not a limiting factor (Archibald et al., 2020). The
680 lack of rain, the high evapotranspiration and the elevated temperatures during the dry
681 season decrease the water availability in the more surficial layers of the soil (Borghetti
682 et al., 2019), resulting in the photosynthetic pigment lost by the herbaceous stratum,
683 while in the rainy season there is an increase in the vegetation reproduction and a
684 concomitant greenness increase (Eamus et al., 2016). Thus, the herbaceous stratum's
685 predominance in the study area and its greater sensitivity to water deficit explain the
686 conspicuous NDVI responses to dry and wet seasons in the savannas.

687

688

689

690

691

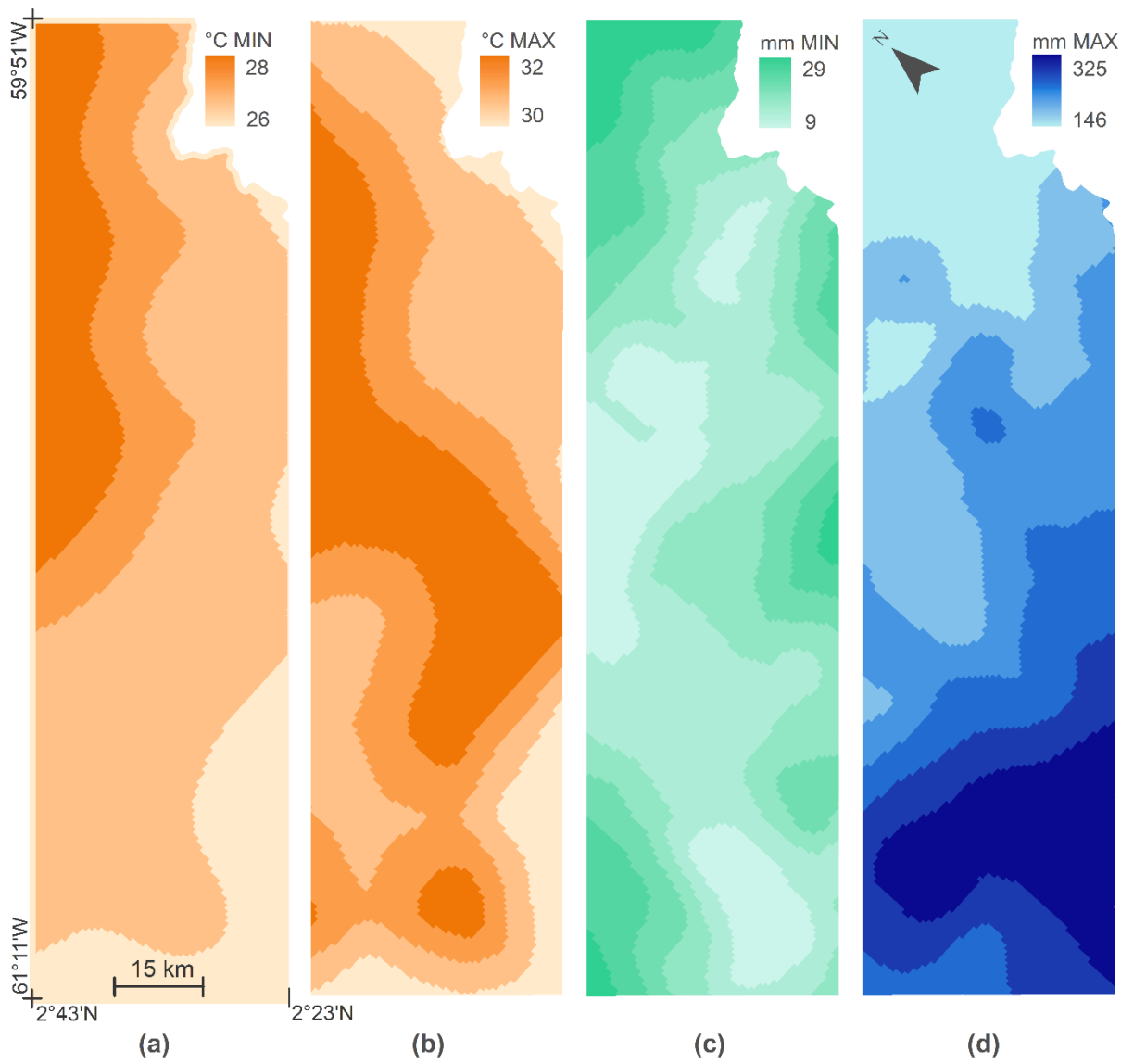
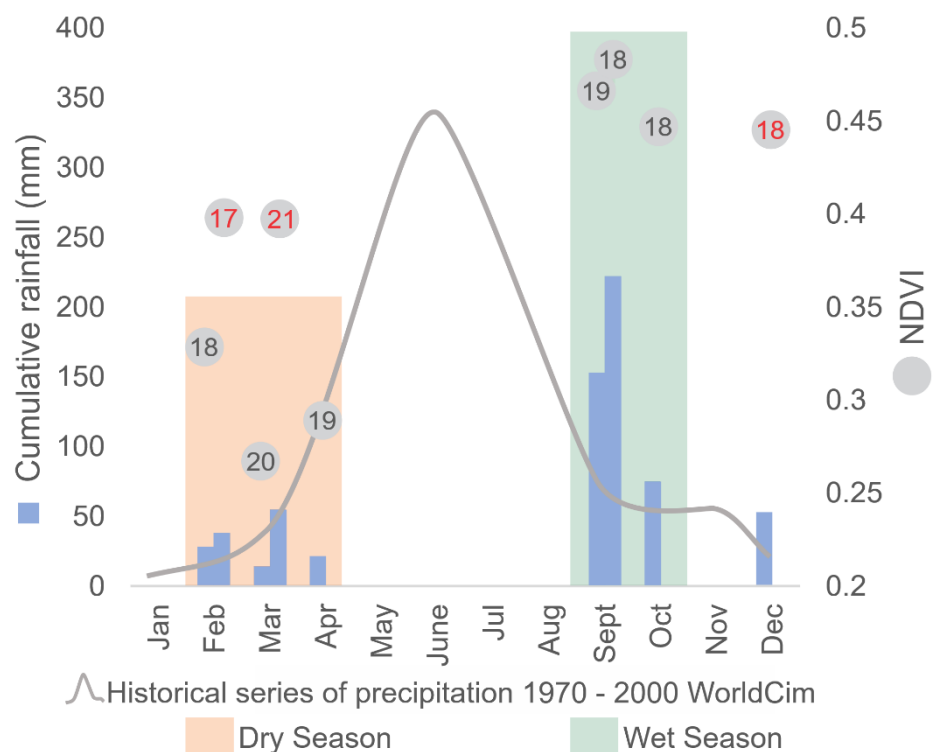


Fig. 8. Average variation of temperature and precipitation over time. (a) The minimum temperature on February 15, 2017. (b) The maximum temperature on April 1, 2019. (c) Minimum accumulated precipitation on March 26, 2020. (d) Maximum accumulated precipitation on September 18, 2018.

693 Fig. 9 shows the NDVI responses related to the climatic seasonality, with the
 694 numbers in circles indicating the image year in the historic series. Generally, low
 695 precipitation values (blue bars) are equivalent to the low NDVI values of the dry
 696 seasons and the high precipitation values are equivalent to the high NDVI values of
 697 the wet seasons. On average, the NDVI was 0.30 in the dry season and 0.47 in the
 698 wet season. The red values indicate the years that showed a different pattern, that is,

699 there was a high NDVI during the dry seasons. In these cases, the precipitation
 700 accumulated in one month was similar to those recorded for the other years ($\Delta P \approx 10$
 701 mm), but when observed the precipitation accumulated in four months, these years
 702 showed significantly higher precipitation values (>100 mm). Finally, important climatic
 703 variables were not considered in this analysis, such as evapotranspiration, La Niña/El
 704 Niño events and consecutive days of drought or rain (Hoyos et al., 2022), could ensure
 705 a greater predictive power than the average and accumulated monthly of the
 706 temperature and precipitation used here.

707



708

Fig. 9. NDVI is controlled by the climatic seasonality (dry and wet seasons). Cumulative rainfall curve derived from historical series from 1970-2000 (Fick and Hijmans, 2017) and monthly cumulative rainfall frequencies (blue bars) for each image date (numbers inside the circles) and the NDVI value associated to each one.

709

710 **3.5. LANDFORMS AND ROCKS**

711 Considering the Slope variable, the area is predominantly smooth, about 92%
712 of its surface has a slope of less than 8%, except for the occasional presence of
713 residual plateaus with slopes higher than 45% (Fig. 10a). For the variable Altitude,
714 values between 75 and 90 m occur in 55% of its extension, while altitudes above 115
715 m appear only in the residual plateaus, making up 6% of the area (Fig. 10b). The
716 coefficient of variation for Landforms and Rocks was 39 and 65, respectively, indicating
717 greater geological variation than geomorphological (Fig. 10c and 10d).

718 On average, landforms showed the following NDVI values: Floodplains (0.56),
719 Planation Surface (0.29), Erosive Planation Surface (0.38), Tucano Hills (0.20),
720 Inselbergs (0.70), and Mountains (0.71). The forest vegetation of structural highs
721 (metamorphic and intrusive rocks) showed NDVI values higher than floodplains. The
722 lower values occurred in the Tucano Hills maybe are perhaps due to the intense rust
723 oxidation of their quartz rich sandstones (Cruz et al., 2019). The high NDVI values of
724 the Erosive Planation Surface are perhaps due to fact that it has higher areas (100 m)
725 and less flooding areas (170 km²) in relation to the Planation Surface (82 m and 518
726 km² respectively).

727 The Rocks variable showed the following NDVI mean values: Areias Brancas
728 Fm (0.28), Boa Vista Fm (0.32), Tucano Fm (0.30), Metamorphics (0.45), Plutonics
729 (0.45), Volcanics (0.32), and Alluvial deposits (0.56). The relations between geologic
730 materials and NDVI don't follow the expected order made here. Contrary to expected,
731 Tucano Fm, and Volcanic areas showed lower NDVI values than Boa Vista Fm. Each
732 of these non-expected results is an average of spatially distinct behaviors within their
733 respective areas. Thus, while the high parts of the Tucano Fm areas showed lower
734 NDVI values, their lower parts showed comparatively higher NDVI values. In contrast,

735 the Vulcanic areas showed high NDVI in the highest altimetric quotas and low in their
736 basin areas. On the other hand, although metamorphic and igneous units showed high
737 NDVI values as expected, perhaps they would show even higher values if a distinction
738 had been made between the lithological types (Urubu and Mucajaí units) associated
739 with the forests in the southwest of the area from those (Cauarane and Saracura units)
740 associated to the savanna in the northeast (Holanda et al., 2014). These discrepancies
741 perhaps are because most of the spatial distribution of each unit is based on
742 interpolations and their nature itself is based on simplistic generalizations of a vast and
743 complex range of lithological types. Large-scale geological surveys and more detailed
744 petrographic and geochemical units would most likely result in more realistic results.

745

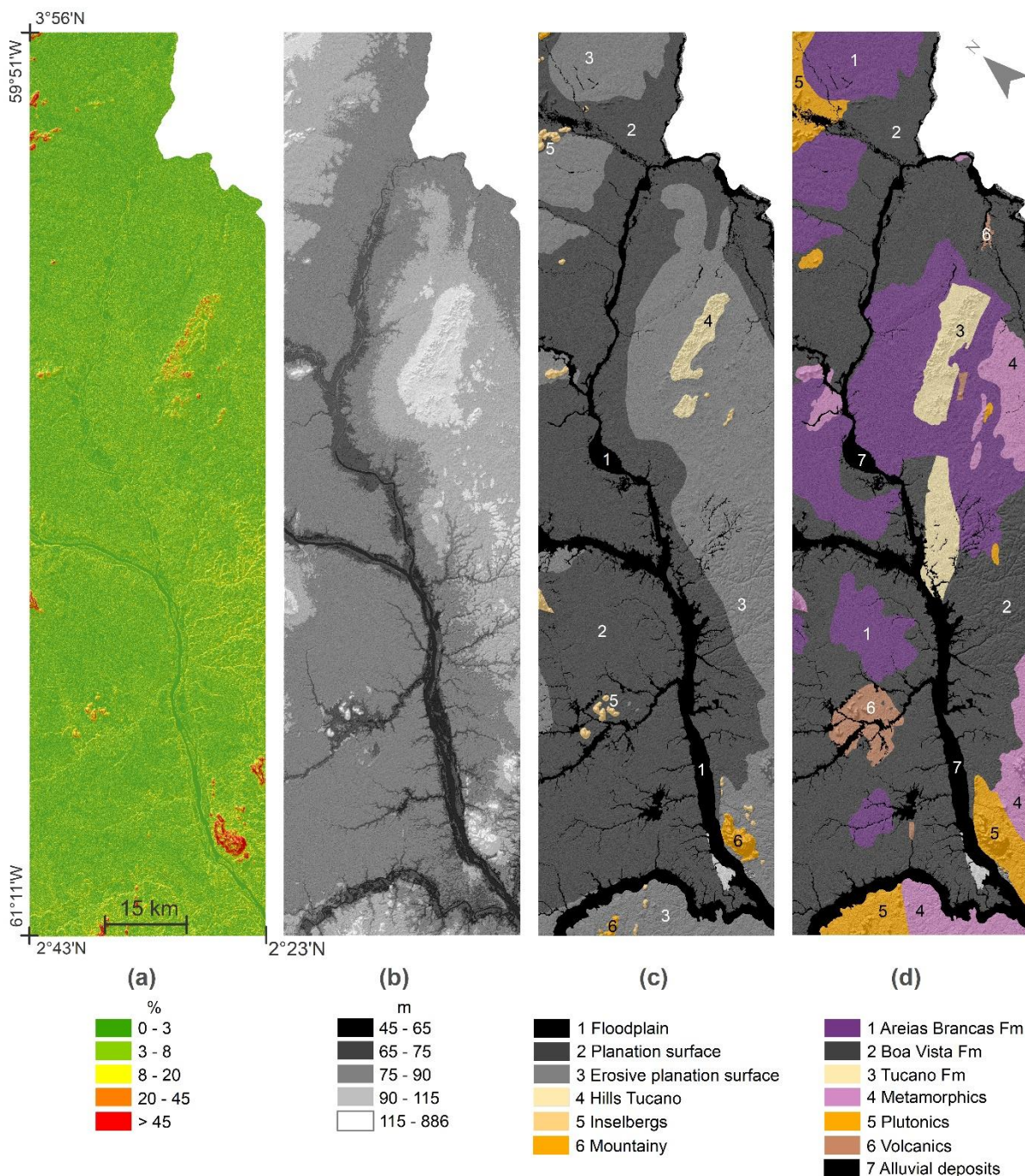


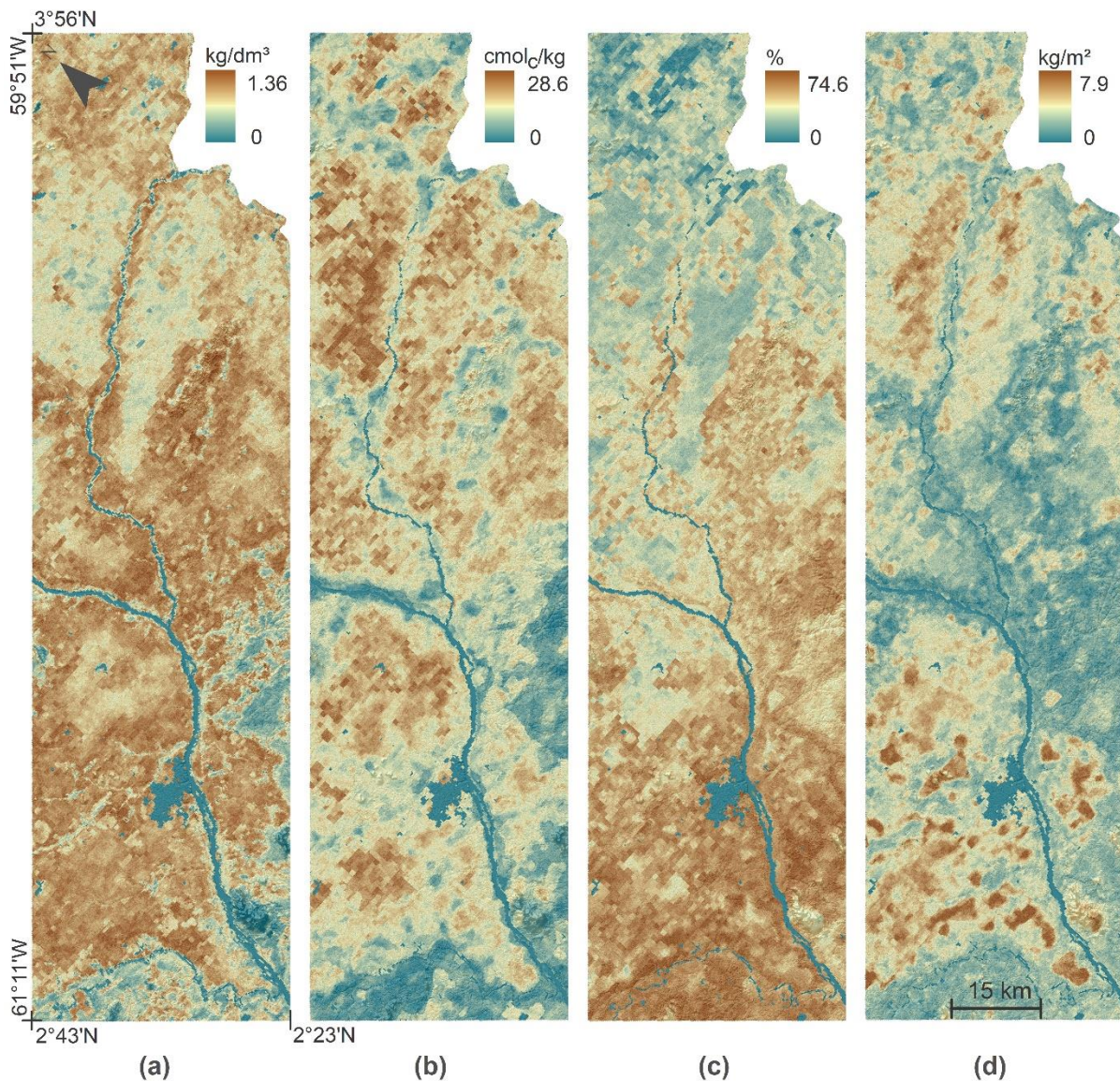
Fig. 10. Spatial distribution of variables (a) Slope, (b) Altitude, (c) Landforms and (d) Rocks.

747 3.6. SOILS PARAMETERS

748 The spatial distribution of soil parameters (Fig. 11) did not vary substantially,
 749 and the mean values and percentage of variation found were: Bulk Density 1.3 kg/dm³
 750 - 3%, CEC 17.7 cmol_c/kg - 20%, Sand 53.2% - 12% and SOCS 4.5 kg/m² - 13%. The
 751 Soilgrids variables reflect the soil characteristics described for the region, the soil Bulk

752 Density are compatible with the values obtained by Feitosa et al. (2016) in field
753 measurements made in savanna and forest patches surfaces, these values tend to
754 increase in subsurface due the cohesive horizons of yellow ferrasols and acrisols (Vale
755 Júnior and Schaefer, 2010). With 53% of sand and 24% of clay, the sandy clay loam
756 texture is due to the source material predominantly sedimentary and are commonly
757 described to the region (Vale Júnior and Schaefer, 2010). The low clay and organic
758 matter content and the hot and humid tropical climate favors weathering and so the
759 soils have low CEC, which is associated to the organic carbon dynamics. The savanna
760 organic carbon dynamics is characterized by a low soil accumulation of organic matter
761 due the lower litter supply, the high decomposition rates, and the sandy soil texture,
762 what results in low SOCS (Simões et al., 2010; Vale Júnior and Sousa, 2005).

763 The Bulk Density is influenced by the amount of organic matter present in the
764 soil. Considering that the organic matter has a density lower than the minerals and acts
765 as a biophysical conditioner to porosity recovering (decreasing the porosity), thus a
766 high density soil implies in low organic matter concentration, and lower carbon input
767 (Ronquim, 2021; Grüneberg et al., 2013).



768

Fig. 11. Spatial distribution of Soilgrids variables (a) Bulk Density (b) CEC. (c) Sand. (d) SOCS.

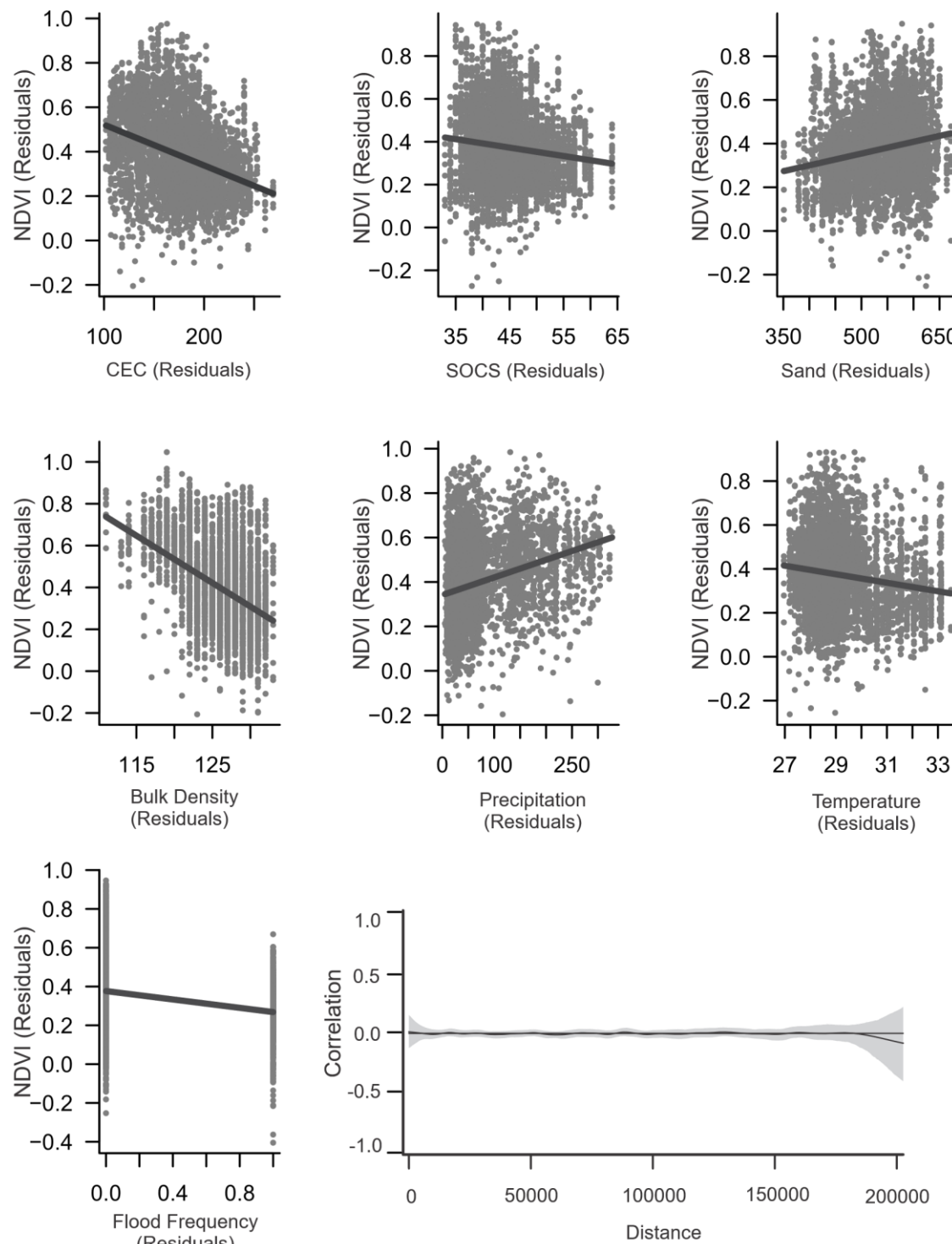
769

770 3.7. SEM

771 The residuals of the linear multiple regression models showed no spatial
 772 autocorrelation, the graphs with the partial regressions of the direct effect on NDVI are
 773 in Fig. 12, where the variable Bulk Density showed the highest correlation. The SEM
 774 revealed that the indirect effects of rocks and landforms on NDVI were 0.33 and 0.16,
 775 respectively (Fig. 13). This result is intrinsically related to the ordering of the groups
 776 within the geology and geomorphology variables. Relief could have been grouped

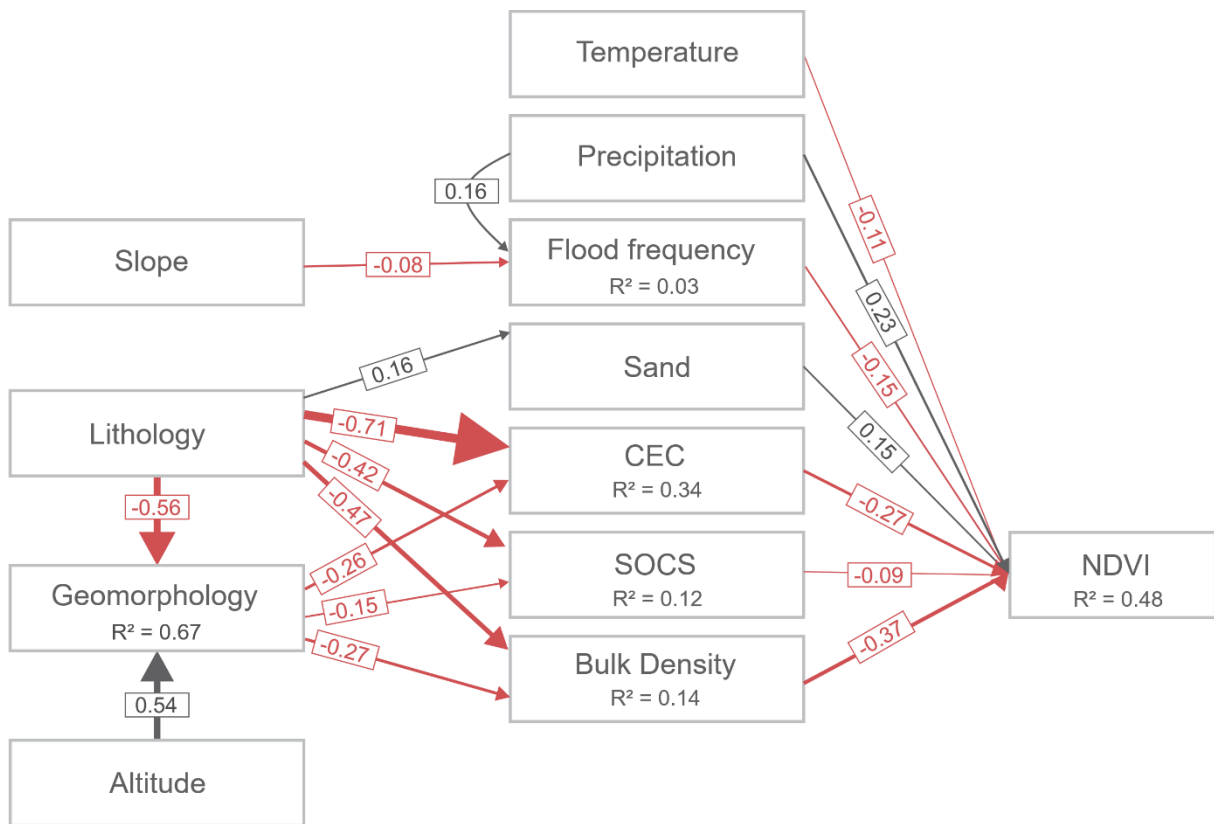
777 based on different combinations of all the characters it represents, however, the
778 number of possible combinations makes this alternative unfeasible for the purposes
779 proposed here. Similarly, the geology variable would be better grouped on a
780 geochemical gradient base, but this is not possible since these data are not available
781 for the scale of the study. Some tests of different ways of ordering were performed
782 here. When grouped by age, the Rock variable lose their indirect effect, i.e., the
783 variation in vegetation showed no relationship to the age of the rocks. Thus, the order
784 presented here was based on the alleged favorability of the geological unit to the
785 development of vegetation and the relief units was ordered by altitude. Rocks showed
786 a greater indirect effect than relief, reinforcing the fact that altitude does not have such
787 a relevant effect. The effect of rocks is due to the relationships between this variable
788 and soils, since rocks are the primary source of macronutrients, and so playing an
789 important role in soil fertility (Gray et al., 2016).

790



791

Fig. 12. Partial regressions of the direct effect on NDVI.



792

Fig. 13. Structural equation model quantifying the direct and indirect effects of abiotic predictors on NDVI. The arrows represent significant ($P < 0.05$), direct and unidirectional relationships between the variables, the arrows that point to other variables before reaching the NDVI express the paths of indirect effects. Black arrows indicate positive effects and red arrows indicate negative effects. The thickness of the arrows is directly proportional to the standardized regression coefficient, that is, to the effect size. R^2 corresponds to the linear models of multiple regressions used in the construction of the SEM.

793

794 As expected, the variables Rocks and Altitude explain much of the landforms
 795 ($R^2=0.67$), but relative to NDVI, altitude had a low indirect effect (0.1), probably
 796 because the area is very smooth and the NASADEM spatial and vertical resolutions is
 797 not so fine to capture such subtle differences in terrain, and/or because the plants are
 798 quite sensitive to the soil hydrological gradients (Cavagnaro, 2016; Silverton et al.,
 799 1999; 2015).

800 Bulk density, CEC and SOCS had negative effects on NDVI, of -0.37, -0.27 and
 801 -0.09, respectively. For the Bulk Density variable this negative effect was expected,

802 since denser soils hinder root development and water infiltration (Vale Júnior and
803 Schaefer, 2010). As for the variables CEC and SOCS, a positive effect was expected,
804 but negative results between vegetal development and these variables are not
805 uncommon (Goodlee et al., 2021; Sana et al., 2014; Silveira et al., 2018). Although the
806 presence of cations in the soil is crucial for the distribution and formation of vegetation
807 (Lloyd et al., 2009), CEC is a measure of how well the soil is able to retain cations, if
808 most of the CEC is occupied by cations essential for plant development, such as
809 calcium, magnesium and potassium, the soil will be fertile, on the other hand, if a large
810 part of the CEC is occupied by potentially toxic cations, such as hydrogen and
811 aluminum, the soil will be poor (Ronquim, 2021). The CEC of Amazonian soils is
812 notoriously occupied by aluminum (Quesada et al., 2011), and high concentrations of
813 hydrogen, and the consequent acidity are described for soils in the studied region (Vale
814 Júnior and Schaefer, 2010). Miranda et al. (2003) reported the influence of these
815 variables on the occurrence and distribution of tree species in the savanna of Roraima.
816 Thus, the negative relationship found here between CEC and NDVI is believed to be
817 due to aluminum toxicity. CEC and SOCS correlate ($R = 0.45$), which may explain the
818 slight negative effect of SOCS on NDVI, when a positive effect would be expected.

819 Regarding the Flood Frequency, slope and precipitation did not explain well this
820 phenomenon ($R^2=0.03$), contrary to the expected. Water flows more on slopes and less
821 on flat land, so the relationship between slope and flooding is negative, here this effect
822 was very small (-0.08) probably because these gradients are very subtle and
823 NASADEM has insufficient resolution to capture them. Precipitation also had a smaller
824 effect on flood frequency (0.16), suggesting that flooded areas are more related to the
825 infiltration capacity of soils, the presence of cohesive horizons, and the level of the
826 water table (Franco et al., 1975).

827 Regarding the NDVI, precipitation showed a positive effect (+0.23) and flood
828 frequency a negative effect (-0.15), both expected results. Precipitation is the principal
829 source of water in the study area, and its effects on vegetation goes beyond simply
830 providing water for plants. The correlation between NDVI and precipitation was 0.27
831 for overall area, 0.32 for non-flooded areas and 0.38 for the flooded areas, while the
832 NDVI on average was higher in the non-flooded areas (0.41) than in those flooded
833 (0.25). These results show that there are minimum and maximum thresholds of
834 precipitated water volume, whose extrapolations imply difficulties for plant
835 development (Tao et al., 2016). Too much water increases the likelihood of the
836 formation of stagnant waters, which reduces oxygen availability to soil microorganisms
837 and plant roots, and can lead to physiological drought, i.e., the inability of roots to
838 absorb resources, so that plants poorly tolerant to flooding suffer marked reductions in
839 photosynthetic capacity and ultimately the intolerant species die (Banach et al., 2009).
840 Too little water, in turn, can cause drought-sensitive plants to lower their metabolism
841 and vigor to avoid reaching the point of permanent wilting (Mosa et al., 2017), and a
842 good example of this is the occurrence in the savannas of Roraima of plants endemic
843 to hydromorphic soils of poorly drained and constantly flooded areas - such as some
844 herbaceous legumes recorded by Cavalcante et al. (2014).

845 Temperature had a small negative effect (-0.11) on NDVI, possibly due to
846 reduction in vegetative productivity to avoid significant water lost with the increased
847 respiration at high temperatures (Sullivan et al., 2020).

848 The positive effect found here between Sand and NDVI (+0.15) can be attributed
849 to the drainage conditions of the soils, in the sense that the greater the amount of sand,
850 the greater its permeability. The hydromorphic character of the soils, that is, long
851 periods of water stagnation followed by dry periods, higher toxicity by exchangeable

852 aluminum and higher acidity are described as hydro-edaphic constraints in field studies
853 in the study area (Araújo et al., 2017; Cavalcante et al., 2014; Feitosa et al., 2016;
854 Xaud and Carvalho, 1999), while better drainage conditions of soils, in the mentioned
855 studies, are associated with forest fragments, wooded savannas, and higher
856 herbaceous legumes species richness and diversities. Together all the direct predictors
857 explain 48% of the variation in NDVI.

858

859 **4. CONCLUSIONS**

860 The NDVI showed 60% of temporal variation through the five years analyzed,
861 responding to climatic seasonality, confirming what was expected. These results are
862 specifically related to the foliar area increase and of the vegetative growth efficiency of
863 their herbaceous elements during the rainy season. Altitude and slope showed no
864 indirect effect on NDVI, while rocks and landforms showed an indirect effect of 0.33
865 and 0.16, respectively. The high value of geology confirmed the validity of the criteria
866 used to order this variable, namely, its favorability to vegetation development based on
867 the probability of inorganic nutrient inputs.

868 The evolutionary history of savannas around the world has conditioned
869 specificities in their abiotic determinants, and in the Amazon the recent sedimentary
870 dynamics have been related to the distribution of vegetation. This study quantified the
871 indirect effect of rocks and reliefs on NDVI, showing that the current landscape
872 configuration in the study area, expressed predominantly by the Sedimentary
873 Formation Boa Vista and the products of its reworking (White Sands Formation and
874 alluvial deposits) arranged in long planing surfaces, resulting from successive cycles
875 of erosion and deposition, punctuated by residual reliefs in the form of inselbergs and
876 mountains, coming mainly from volcanic rocks of the pre-rift phase of the Tacutu

877 Sedimentary Basin and from crystalline and metamorphic rocks, even older, of the
878 Guiana Shield, contributes to the distribution of savannas, that is, the evolutionary
879 history of this landscape has an indirect effect on the variation of NDVI.

880 Considering the variables with direct effect on NDVI, a strong positive effect was
881 expected with the indicators of soil fertility (CEC and SOCS), but the relationship was
882 negative because the soils are acidic and with high exchangeable aluminum. A
883 stronger effect of moisture-related predictors (precipitation and flooding frequency)
884 than of soil-related predictors was expected, as occurs in savannas on a global scale,
885 but this was not confirmed. Although flooding has a negative effect and precipitation a
886 positive effect, this is a complex relationship, given the presence of herbaceous-shrub
887 matrix with hygrophytes elements specially adapted for soil hypersaturation conditions.
888 Thus, precipitation and flood frequency did not have a high effect as the soil variables,
889 but the soil variable with the highest effect is Bulk Density, which is precisely linked to
890 water drainage in soils. The positive effect of the concentration of sand reinforces the
891 hydroedaphic restrictions; periodically flooded areas hinder the establishment of tree
892 species, which is favored in areas with better drainage conditions.

893

894 **5. ACKNOWLEDGMENTS**

895 Bruna Mendel received a master's scholarship from the Coordenação de
896 Aperfeiçoamento de Pessoal de Nível Superior (CAPES) during the course of this
897 study.

898

899 **6. REFERENCES**

- 900 Albert, J. S., Val, P., Hoorn, C. (2018). The changing course of the Amazon River in the Neogene: center
901 stage for Neotropical diversification. *Neotropical Ichthyology*, 16.
902 ANA. Agência Nacional de Águas HIDROWEB v3.1.1. Accessed through <<http://www.snh.gov.br/hidroweb/serieshistoricas>>. Access in: mar. 2020.
903

- 904 Araújo, M. A. M., Rocha, A. E. S. D., Miranda, I. D. S., Barbosa, R. I. (2017). Hydro-edaphic conditions
 905 defining richness and species composition in savanna areas of the northern Brazilian Amazonia.
 906 *Biodiversity Data Journal*, (5), e13829.
- 907 Araújo Júnior, A. C. R., Tavares Júnior, S. S. (2017). Land use and cover for urban planning, Boa Vista,
 908 Roraima, Brasil. *Boletim Goiano de Geografia* 37(1), 36-55.
- 909 Archibald, S., Bond, W. J., Hoffmann, W., Lehmann, C., Staver, C., Stevens, N. (2019). Distribution and
 910 determinants of savannas. *Savanna woody plants and large herbivores*, 1-24.
- 911 Banach, K., Banach, A. M., Lamers, L. P., De Kroon, H., Bennicelli, R. P., Smits, A. J., Visser, E. J.
 912 (2009). Differences in flooding tolerance between species from two wetland habitats with contrasting
 913 hydrology: implications for vegetation development in future floodwater retention areas. *Annals of*
 914 *botany*, 103(2), 341-351.
- 915 Barbosa, R. I. (1997). Distribuição das chuvas em Roraima. In: Barbosa, R. I., Ferreira, E. F. G., Cas-
 916 tellon, E. G. (Eds.), *Homem, Ambiente e Ecologia no Estado de Roraima*. Editora INPA, Manaus,
 917 Amazonas, pp. 325-335.
- 918 Barbosa, R. I., Campos, C. (2011). Detection and geographical distribution of clearing areas in the sa-
 919 vannas ('Lavrado') of Roraima using Google Earth web tool. *Journal of Geography and Regional*
 920 *Planning*, 4(3): 122-136.
- 921 Barbosa, R. I., Campos, C., Pinto, F., Fearnside, P. M. (2007). The "Lavrados" of Roraima: biodiversity
 922 and conservation of Brazil's Amazonian Savannas. *Functional Ecosystems and Communities*, 1(1),
 923 29-41.
- 924 Barbosa, R. I., Miranda, I. D. S. (2005). Fitofisionomias e diversidade vegetal das savanas de Roraima.
 925 *Savanias de Roraima: Etnoecologia, Biodiversidade e Potencialidades Agrossilvipastoris*, FEMACT,
 926 Boa Vista, 61-77.
- 927 Bardgett, R. D., Bullock, J. M., Lavorel, S., Manning, P., Schaffner, U., Ostle, N., ... Shi, H. (2021).
 928 Combatting global grassland degradation. *Nature Reviews Earth & Environment*, 2(10), 720-735.
- 929 Barni, P. E., Barbosa, R. I., Xaud, H. A. M., Xaud, M. R., Fearnside, P. M. (2022). Precipitation in north-
 930 ern Amazonia: spatial distribution in Roraima, Brazil. *Sociedade & Natureza*, 32, 420-436.
- 931 BDIA Banco de dados de informações ambientais IBGE. Accessed through
 932 <<https://bdiaweb.ibge.gov.br/#/home>>. Access in: jan. 2021.
- 933 Beaudoin, H., Rodell, M. NASA/GSFC/HSL (2020). GLDAS Noah Land Surface Model L4 3 hourly
 934 0.25 x 0.25 degree V2.1, Greenbelt, Maryland, USA, Goddard Earth Sciences Data and Information
 935 Services Center (GES DISC).
- 936 Benedetti, U. G., Vale Júnior, J. F. D., Schaefer, C. E. G. R., Melo, V. F., Uchôa, S. C. P. (2011). Gênese,
 937 química e mineralogia de solos derivados de sedimentos plioleistocênicos e de rochas vulcânicas
 938 básicas em Roraima, Norte Amazônico. *Revista Brasileira de Ciência do Solo*, 35(2), 299-312.
- 939 Bond, W. J. (2010). Do nutrient-poor soils inhibit development of forests? A nutrient stock analysis. *Plant*
 940 *and soil*, 334(1), 47-60.
- 941 Borghetti, F., Barbosa, E., Ribeiro, L., Ribeiro, J. F., Walter, B. M. T. (2019). South American Savannas.
 942 *Savanna Woody Plants and Large Herbivores*, 77-122.
- 943 Carrijo, J. N., Maracahipes, L., Scalón, M. C., Silvério, D. V., Abadia, A. C., Fagundes, M. V., ... Lenza,
 944 E. (2021). Functional traits as indicators of ecological strategies of savanna woody species under
 945 contrasting substrate conditions. *Flora*, 284, 151925.
- 946 Carvalho, T. M., Maia, R. P., Sander, C. (2021). Inserção do rio Branco nas áreas úmidas da Amazônia,
 947 estado de Roraima, Amazônia Setentrional.
- 948 Cavagnaro, T. R. (2016). Soil moisture legacy effects: impacts on soil nutrients, plants and mycorrhizal
 949 responsiveness. *Soil Biology and Biochemistry*, 95, 173-179.
- 950 Cavalcante, C. D. O., Flores, A. S., Barbosa, R. I. (2014). Edaphic factors determining the occurrence
 951 of herbaceous legumes in Amazonian savannas. *Acta Amazonica*, 44, 379-386.

- 952 Cediel, F., Shaw, R. P., Cceres, C. (2003). Tectonic assembly of the northern Andean block.
- 953 Charlton, R. (2007). Fundamentals of fluvial geomorphology. Routledge.
- 954 Cordeiro, C. L., Rossetti, D. F., Gribel, R., Tuomisto, H., Zani, H., Ferreira, C. A., Coelho, L. (2016).
955 Impact of sedimentary processes on white-sand vegetation in an Amazonian megafan. *Journal of
956 Tropical Ecology*, 32(6), 498-509.
- 957 Costa, J. A. V., Falcão, M. T. (2011). Compartimentação morfotectônica e implicações de evolução do
958 relevo do hemigráben do Tacutu no Estado de Roraima. *Revista Brasileira de Geomorfologia*, 12(1).
- 959 Costa, N. D. L., Moraes, A., Gianluppi, V., Bendahan, A. B. (2014). Avaliação da rebrota natural de
960 pastagens de *Trachypogon plumosus* nos cerrados de Roraima. *Scientia Agraria Paranaensis*,
961 13(1), 57-64.
- 962 Costa, N. D. L., Gianluppi, V., Moraes, A., Bendahan, A. B. (2011). Produtividade de forragem e carac-
963 terísticas morfogênicas e estruturais de *Axonopus aureus* nos cerrados de Roraima. *Amazônia Ciên-
964 cia & Desenvolvimento*, 6(12), 7-22.
- 965 Crawford, F. D., Szelewski, C. E. (1984). Geology and exploration in the Takutu graben of Guyana. *Oil
966 & gas journal*, 82(10): 122-129.
- 967 Crawford, F. D., Szelewski, C. E., Alvey, G. D. (1985). Geology and exploration in the Takutu graben of
968 Guyana Brazil. *Journal of Petroleum Geology*, 8(1): 5-36.
- 969 Cremon, É. H., de Fátima Rossetti, D., de Oliveira Sawakuchi, A., Cohen, M. C. L. (2016). The role of
970 tectonics and climate in the late Quaternary evolution of a northern Amazonian River. *Geomorphol-
971 ogy*, 271, 22-39.
- 972 Crippen, R. E., Buckley, S., Agram, P. S., Belz, J. E., Gurrola, E. M., Hensley, S., ... Tung, W. (2016).
973 NASADEM global elevation model of earth: Methods for the refinement and merger of SRTM and
974 ASTER GDEM. In *AGU Fall Meeting Abstracts* (Vol. 2016, pp. IN43B-1692).
- 975 Cruz, C. M., Holanda, E. C., Evangelista, T. A. (2019). Composição florística do cretáceo inferior da
976 Formação Serra do Tucano, Bacia do Tacutu, RR. In: *Anais Do Xxvi Congresso Brasileiro De Pale-
977 ontologia. Anais eletrônicos...* Galoá. Accessed through <<https://proceedings.science/cbp-2019/papers/composicao-floristica-do-cretaceo-inferior-da-formacao-serra-do-tucano--bacia-do-tacutu--rr?lang=en>>. Access in jun. 2021.
- 980 D'Addabbo, A., Refice, A., Pasquariello, G., Lovergne, F. (2016). SAR/optical data fusion for flood de-
981 tection. In *2016 IEEE International Geoscience and Remote Sensing Symposium (IGARSS)* (pp.
982 7631-7634). IEEE.
- 983 Diniz, A.M.A., Lacerda, E.G. (2018). The complexities of the Brazilian Amazon frontier and its most
984 recent chapter: soybean expansion in Roraima. In.: Roy Jones and Alexandre M. A. Diniz, *Twentieth
985 Century Land Settlement Schemes*, (1st ed.), NY: Routledge, pp: 178-204
- 986 Drucker, D. P., Costa, F. R. C., Magnusson, W. E. (2008). How wide is the riparian zone of small streams
987 in tropical forests? A test with terrestrial herbs. *Journal of Tropical Ecology*, 24(1), 65-74.
- 988 Eamus, D., Huete, A., Yu, Q. (2016). Savannas. In *Vegetation Dynamics: A Synthesis of Plant Ecophys-
989 iology, Remote Sensing and Modelling* (pp. 383-414). Cambridge: Cambridge University Press.
- 990 Eiras, J. F., Kinoshita, E. M. (1990). *Geologia e perspectivas petrolíferas da Bacia do Tacutu. Origem e
991 Evolução das Bacias Sedimentares*: PETROBRAS, Anais, 197-220.
- 992 Empresa Brasileira De Pesquisa Agropecuária – EMBRAPA. (1979). Serviço Nacional de Levanta-
993 mento e Conservação de Solos. In: *Reunião Técnica De Levantamento De Solos. Súmula...Rio de
994 Janeiro*. 83p.
- 995 FAO. (2015). World Reference Base for Soil Resources 2014, update 2015 International soil classifica-
996 tion system for naming soils and creating legends for soil maps. *World Soil Resources Reports No.
997 106. IUSS Working Group WRB*, Rome.
- 998 ESA. (2018). *Sentinel-2 User Guide*. Accessed through <<https://sentinel.esa.int/web/sentinel/technical-guides/sentinel-2-msi>>. Access in jan. 2020.

- 1000 Farr, T. G., Rosen, P. A., Caro, E., Crippen, R., Duren, R., Hensley, S., ... Alsdorf, D. (2007). The shuttle
 1001 radar topography mission. *Reviews of geophysics*, 45(2).
- 1002 Feitosa, K. K. A., Vale Júnior, J. F. D., Schaefer, C. E. G. R., Sousa, M. I. L. D., Nascimento, P. P. R.
 1003 R. (2016). Relações solo-vegetação em "ilhas" florestais e savanas adjacentes, no nordeste de Ro-
 1004 raima. *Ciência Florestal*, 26(1), 135-146.
- 1005 Fernandes, G.W. Coelho, M.S. Machado, R.B. Ferreira, M.E. Aguiar, L.M.S. Dirzo, R. Scariot, A., Lopes,
 1006 C.R. (2016). Afforestation of savannas: an impending ecological disaster. *Brazilian Journal of Nature
 1007 Conservation*, 14: 146-151.
- 1008 Ferreira, C. S., Carmo, W. S. D., Graciano-Ribeiro, D., Oliveira, J. M. F. D., Melo, R. B. D., Franco, A.
 1009 C. (2015). Leaf anatomy of eleven dominant woody species in the savannas of Roraima. *Acta Ama-
 1010 zonica*, 45, 337-346.
- 1011 Fick, S. E., Hijmans, R. J. (2017). WorldClim 2: new 1-km spatial resolution climate surfaces for global
 1012 land areas. *International journal of climatology*, 37(12), 4302-4315.
- 1013 Furlan, L. M., Rosolen, V., Salles, J., Moreira, C. A., Ferreira, M. E., Bueno, G. T., ... Mounier, S. (2020).
 1014 Natural superficial water storage and aquifer recharge assessment in Brazilian savanna wetland us-
 1015 ing unmanned aerial vehicle and geophysical survey. *Journal of Unmanned Vehicle Systems*, 8(3):
 1016 224-244.
- 1017 Franco, E. M. S., Del'arco, J. O., Rivetti, M. (1975). Folha NA. 20 Boa Vista e parte das Folhas NA. 21
 1018 Tumucumaque, NB. 20 Roraima e NB. 21. Geomorfologia. BRASIL. Projeto RADAMBRASIL. Geo-
 1019 morfologia. Rio de Janeiro. DNPM, 139-180.
- 1020 Godlee, J. L., Ryan, C. M., Bauman, D., Bowers, S. J., Carreiras, J. M., Chisingui, A. V., ... Dexter, K.
 1021 G. (2021). Structural diversity and tree density drives variation in the biodiversity–ecosystem function
 1022 relationship of woodlands and savannas. *New Phytologist*, 232(2), 579-594.
- 1023 Gray, J. M., Bishop, T. F., Wilford, J. R. (2016). Lithology and soil relationships for soil modelling and
 1024 mapping. *Catena*, 147: 429-440.
- 1025 Grohmann, C. H. (2018). Evaluation of TanDEM-X DEMs on selected Brazilian sites: Comparison with
 1026 SRTM, ASTER GDEM and ALOS AW3D30. *Remote Sensing of Environment*, 212, 121-133.
- 1027 Grüneberg, E., Schöning, I., Hessenmöller, D., Schulze, E. D., Weisser, W. W. (2013). Organic layer
 1028 and clay content control soil organic carbon stocks in density fractions of differently managed Ger-
 1029 man beech forests. *Forest Ecology and Management*, 303, 1-10.
- 1030 Guisan, A., Zimmermann, N. E. (2000). Predictive habitat distribution models in ecology. *Ecological
 1031 modelling*, 135(2-3), 147-186.
- 1032 Gurgel, H. D. C., Ferreira, N. J., Luiz, A. J. (2003). Estudo da variabilidade do NDVI sobre o Brasil,
 1033 utilizando-se a análise de agrupamentos. *Revista Brasileira de Engenharia Agrícola e Ambiental*,
 1034 7(1), 85-90.
- 1035 Hahn, P. Y. S., Júnior, S. S. T., Neta, L. C. B., Gauger, A. P. (2012). Caracterização das unidades
 1036 morfoestruturais do Hemigraben Tacutu, Norte de Roraima. *Revista Geonorte*, 3(5), 1378-1383.
- 1037 Hengl, T., Mendes de Jesus, J., Heuvelink, G. B., Ruiperez Gonzalez, M., Kilibarda, M., Blagotić, A., ...
 1038 Kempen, B. (2017). SoilGrids250m: Global gridded soil information based on machine learning.
 1039 *PLoS one*, 12(2), e0169748.
- 1040 Higgins, M. A., Ruokolainen, K., Tuomisto, H., Llerena, N., Cardenas, G., Phillips, O. L., ... Räsänen, M.
 1041 (2011). Geological control of floristic composition in Amazonian forests. *Journal of biogeography*,
 1042 138(11), 2136-2149.
- 1043 Hill MJ. (2021). Remote Sensing of Savannas and Woodlands: Editorial. *Remote Sensing*. 13(8):1490.
- 1044 Hoffmann, W. A., Geiger, E. L., Gotsch, S. G., Rossatto, D. R., Silva, L. C., Lau, O. L., ... Franco, A. C.
 1045 (2012). Ecological thresholds at the savanna-forest boundary: how plant traits, resources and fire
 1046 govern the distribution of tropical biomes. *Ecology letters*, 15(7), 759-768.
- 1047 Holanda, J. L. R., Marmos, J. L., Maia, M. A. M. (2014). Geodiversidade do estado de Roraima. CPRM.

- 1048 Holben, B. N., Shimabukuro, Y. E. (1993). Linear mixing model applied to coarse spatial resolution data
1049 from multispectral satellite sensors. *Remote Sensing*, 14(11), 2231-2240.
- 1050 Hoyos, N., Correa-Metrio, A., Jaramillo, C., Villegas, J. C., Escobar, J. (2022). Effects of consecutive
1051 dry and wet days on the forest–savanna boundary in north-west South America. *Global Ecology and
1052 Biogeography*, 31(2), 347-361.
- 1053 IBGE (2009). Manual Técnico da Geomorfologia Brasileira. Rio de Janeiro, 2.
- 1054 IBGE (2012). Manual Técnico da Vegetação Brasileira. Rio de Janeiro, 1.
- 1055 Kulkarni, S. C., Rege, P. P. (2020). Pixel level fusion techniques for SAR and optical images: A review.
1056 *Information Fusion*, 59, 13-29.
- 1057 Ladeira, L. F. B., Dantas, M. E. (2014). Compartimentação geomorfológica. Holanda, Jl.
- 1058 Latrubblesse, E. M., Nelson, B. W. (2001). Evidence for Late Quaternary aeolian activity in the Roraima–
1059 Guyana region. *Catena*, 43(1), 63-80.
- 1060 Lehmann C.E.R., Parr C.L. (2016). Tropical grassy biomes: linking ecology, human use and conserva-
1061 tion. *Phil. Trans. R. Soc. B* 371: 20160329.
- 1062 Lehmann, C. E., Anderson, T. M., Sankaran, M., Higgins, S. I., Archibald, S., Hoffmann, W. A., ... Bond,
1063 W. J. (2014). Savanna vegetation-fire-climate relationships differ among continents. *Science*,
1064 343(6170), 548-552.
- 1065 Lehmann, C. E., Archibald, S. A., Hoffmann, W. A., Bond, W. J. (2011). Deciphering the distribution of
1066 the savanna biome. *New Phytologist*, 191(1), 197-209.
- 1067 Lima, M.S.B. (2020). Expansão da cadeia da soja na Amazônia Setentrional: os casos de Roraima e
1068 Amapá. *Boletim de Geografia da Universidade Estadual de Maringá*, 38(2): 79-93.
- 1069 Lloyd J, Goulden ML, Ometto JP, Patiño S, Fyllas NM, Quesada CA. (2009). Ecophysiology of forest
1070 and savanna vegetation. In *Amazonia and global change* (eds Keller M, Bustamante M, Gash J,
1071 Silva Dias P), pp. 463–484. Washington, DC: American Geophysical Union.
- 1072 Lloyd, J., Bird, M. I., Vellen, L., Miranda, A. C., Veenendaal, E. M., Djagbletey, G., ... Farquhar, G. D.
1073 (2008). Contributions of woody and herbaceous vegetation to tropical savanna ecosystem produc-
1074 tivity: a quasi-global estimate. *Tree physiology*, 28(3), 451-468.
- 1075 Macintyre, P., Van Niekerk, A., Mucina, L. (2020). Efficacy of multi-season Sentinel-2 imagery for com-
1076 positional vegetation classification. *International Journal of Applied Earth Observation and Geoinfor-
1077 mation*, 85, 101980.
- 1078 Magnusson, W. E., Mourão, G., Costa, F. R. C. (2015). Estatística sem matemática: a ligação entre as
1079 questões e as análises.
- 1080 Mahyouba, S., Fadilb, A., Mansour, E. M., Rhinanea, H., Al-Nahmia, F. (2019). Fusing of optical and
1081 synthetic aperture radar (SAR) remote sensing data: A systematic literature review (SLR). *Interna-
1082 tional Archives of the Photogrammetry, Remote Sensing and Spatial Information Sciences*,
1083 42(4/W12), 127-138.
- 1084 MapBiomas (2022). Statistics. Accessed through <<https://mapbiomas.org/en/statistics>>. Access in fev.
1085 2022.
- 1086 Matías, L., Hidalgo-Galvez, M. D., Cambrollé, J., Domínguez, M. T., Pérez-Ramos, I. M. (2021). How
1087 will forecasted warming and drought affect soil respiration in savannah ecosystems? The role of tree
1088 canopy and grazing legacy. *Agricultural and Forest Meteorology*, 304, 108425.
- 1089 Meneses, M. E. N. D. S., Costa, M. L. D. (2012). Caracterização mineralógica e química dos regolitos
1090 de uma área de transição savana-floresta em Roraima: uma análise da evolução da paisagem.
- 1091 Meneses, M. E. N. D. S., Costa, M. L. D., Costa, J. A. V. (2007). Os lagos do lavrado de Boa Vista-
1092 Roraima: fisiografia, físico-química das águas, mineralogia e química dos sedimentos. *Brazilian
1093 Journal of Geology*, 37(3), 478-489.

- 1094 Meneses, P. R., Almeida, T. D. (2012). Introdução ao processamento de imagens de sensoriamento
1095 remoto. Universidade de Brasília, Brasília.
- 1096 Menezes, F. B., Wankler, F. L. (2020). Sistemas deposicionais fluviais: análise estratigráfica das unida-
1097 des sedimentares da Formação Boa Vista, nordeste da bacia do Tacutu, RR. Revista Geográfica
1098 Acadêmica, 14(1), 69-93.
- 1099 Miall, A. D. (2006). The Geology of Fluvial Deposits. Sedimentary Facies, Basin Analysis, and Petroleum
1100 Geology. Berlin: Springer, 4th. ed., 599 pp.
- 1101 Milani, E.J., Thomaz Filho, A. (2000). Sedimentary Basins of South America. In: Cordani, U.G., Milani,
1102 E.J., Thomaz Filho, A. Campos, D.A. (eds.). Tectonic Evolution of South America. Rio de Janeiro,
1103 31st. IGC, 389-449.
- 1104 Miller, G. R., Cable, J. M., McDonald, A. K., Bond, B., Franz, T. E., Wang, L., ... Scott, R. L. (2012).
1105 Understanding ecohydrological connectivity in savannas: a system dynamic modelling approach.
1106 Ecohydrology, 5(2), 200-220.
- 1107 Miranda, I. S., Absy, M. L. (2000). Fisionomia das savanas de Roraima, Brasil. Acta Amazonica, 3, 423-
1108 440.
- 1109 Miranda, I. S., Absy, M. L., Rebêlo, G. H. (2003). Community structure of woody plants of Roraima
1110 savannahs, Brazil. Plant Ecology, 164(1), 109-123.
- 1111 Misra, G., Cawkwell, F., Wingler, A. (2020). Status of phenological research using Sentinel-2 data: A
1112 review. Remote Sensing, 12(17), 2760.
- 1113 Mistry, J., Beradi, A. (2000). The Savanna ecosystem. In.: J. Mistry and A. Beradi (eds.), World Savan-
1114 nas - Ecology and Human Use, Routledge Ed., 1st. ed., NY, USA, 1-25 pp.
- 1115 Montalvão, R. M. G., Muniz, M. B., Issler, R. S., Dall'Agnol, R., Lima, M. I. C., Fernandes, P. E. C. A.,
1116 Silva, G. G. (1975). Folha NA. 20 Boa Vista e parte das Folhas NA. 21 Tumucumaque, NB. 20
1117 Roraima e NB. 21. Geoogia. BRASIL. Projeto RADAMBRASIL. Geomorfologia. Rio de Janeiro.
1118 DNPM, 15-136.
- 1119 Moreira, A. (2013). Synthetic aperture radar (SAR): Principles and applications.
- 1120 Mosa, K. A., Ismail, A., & Helmy, M. (2017). Plant stress tolerance: an integrated omics approach. Cham:
1121 Springer, 1-19.
- 1122 Helmy, M. (2017). Introduction to plant stresses. In Plant stress tolerance (pp. 1-19). Springer, Cham.
- 1123 Mudd, S. M. (2020). Topographic data from satellites. In Developments in Earth Surface Processes (Vol.
1124 23, pp. 91-128). Elsevier.
- 1125 Murphy, B. P., Bowman, D. M. (2012). What controls the distribution of tropical forest and savanna?
1126 Ecology letters, 15(7), 748-758.
- 1127 Nascimento, S. O., Junior, S. T., Neta, L. B. (2014). Mapeamento geomorfológico da região do Gráben
1128 do Tacutu, por meio de análise de morfoestruturas. Revista Geonorte, 5(16), 218-224.
- 1129 Oliveras, I., Malhi, Y. (2016). Many shades of green: the dynamic tropical forest–savannah transition
1130 zones. Philosophical Transactions of the Royal Society B: Biological Sciences, 371(1703),
1131 20150308.
- 1132 Oliveira, P. C., Parolin, P., Borghetti, F. (2019). Can germination explain the distribution of tree species
1133 in a savanna wetland? Austral Ecology, 44(8), 1373-1383.
- 1134 PALSAR (2015). Radiometric Terrain Corrected low res Includes Material © JAXA/METI 2007. Ac-
1135 cessed through <<https://ASF.alaska.edu/>>. Access in: jan. 2020.
- 1136 Pennington, R. T., Lehmann, C. E. R. Rowland, L. (2018). Tropical savannas and dry forests. Current
1137 Biology, 28, pp: R527-R548.

- 1138 Pennington, R. T., Lewis, G. P. Ratter, J. A. (2006). An overview of the plant diversity, biogeography
 1139 and conservation of Neotropical Savannas and seasonally dry forests. In.: R. Toby Pennington and
 1140 James A. Ratter (eds.), 1st. ed., Boca Raton FL: CRC Press, pp 1-30.
- 1141 Petri, C. A., Galvão, L. S., Lyapustin, A. I. (2019). MODIS BRDF effects over Brazilian tropical forests
 1142 and savannahs: A comparative analysis. *Remote Sensing Letters*, 10(2), 95-102.
- 1143 Pierdicca, N., Pulvirenti, L., Chini, M., Guerriero, L., Candela, L. (2013). Observing floods from space:
 1144 Experience gained from COSMO-SkyMed observations. *Acta Astronautica*, 84, 122-133.
- 1145 Pivello, V. R. (2011). The use of fire in Cerrado and Amazonian Rainforests of Brazil: Past and Present.
 1146 *Fire Ecology*, 7(1): 24-39.
- 1147 Quesada, C. A., Lloyd, J., Anderson, L. O., Fyllas, N. M., Schwarz, M., Czimczik, C. I. (2011). Soils of
 1148 Amazonia with particular reference to the RAINFOR sites. *Biogeosciences*, 8(6), 1415-1440.
- 1149 Ramos, I. M. P., Álvarez-Méndez, A., Wald, K., Matías, L., Hidalgo-Galvez, M. D., Navarro-Fernández,
 1150 C. M. (2021). Direct and indirect effects of global change on mycorrhizal associations of savanna
 1151 plant communities. *Oikos*, 130(8), 1370-1384.
- 1152 R Core Team (2013) R: A language and environment for statistical computing. R Foundation for Statis-
 1153 tical Computing.
- 1154 Ratnam, J., Bond, W. J., Fensham, R. J., Hoffmann, W. A., Archibald, S., Lehmann, C. E., ... Sankaran,
 1155 M. (2011). When is a 'forest'a savanna, and why does it matter? *Global Ecology and Biogeography*,
 1156 20(5), 653-660.
- 1157 Reis, N. J., Nunes, N. D. V., Pinheiro, S. D. S. (1994). A Cobertura Mesozóica do Hemigraben Tacutu-
 1158 Estado de Roraima. Uma abordagem ao Paleo-ambiente da Formação Serra do Tucano. SBG,
 1159 Congr. Bras. Geol, 38, 234-235.
- 1160 Reis, N. J., Faria, M. D., Maia, M. A. M. (2001). O quadro Cenozoico da porção norte-oriental do Estado
 1161 de Roraima. Contribuição à Geologia da Amazônia, 3, 259-272.
- 1162 Reis, N. J., Szatmari, J., Wanderley Filho, J. R., York, D., Evensen, N. M., Smith, P. E. (2006). Dois
 1163 eventos de magmatismo máfico mesozóico na fronteira Brasil-Guiana, escudo das Guianas: enfo-
 1164 que à região do rifte Tacutu-North Savannas. SBG, Congr. Bras. Geol., 43, 459-464.
- 1165 Ronquim, C. C. (2021). Fertility concepts and adequate management for soils in tropical regions. Em-
 1166 brapa Territorial-Boletim de Pesquisa e Desenvolvimento (INFOTECA-E).
- 1167 Rosim, S., Monteiro, A. M. V., Rennó, C. D., Oliveira, J. R. F. (2008). Uma ferramenta open source que
 1168 unifica representações de fluxo local para apoio à gestão de recursos hídricos no Brasil. IP. Infor-
 1169 mática Pública, 10, 29-49.
- 1170 Rosim, S., Monteiro, A. M. V., Rennó, C. D., Souza, R. D., Soares, J. V. (2003). TerraHidro - Uma
 1171 plataforma computacional para o desenvolvimento de aplicativos para a análise integrada de recur-
 1172 sos hídricos. XI Simpósio Brasileiro de Sensoriamento Remoto-SBSR, 2589-2596.
- 1173 Rossetti, D. F., Gribel, R., Cohen, M. C. L., Valeriano, M. M., Tatumi, S. H., Yee, M. (2019a). The role
 1174 of Late Pleistocene-Holocene tectono-sedimentary history on the origin of patches of savanna veg-
 1175 etation in the middle Madeira River, southwest of the Amazonian lowlands. *Palaeogeography, Palae-
 1176 oeclimatology, Palaeoecology*, 526, 136-156.
- 1177 Rossetti, D. F., Moulatlet, G. M., Tuomisto, H., Gribel, R., Toledo, P. M., Valeriano, M. M., ..., Ferreira,
 1178 C. A. (2019b). White sand vegetation in an Amazonian lowland under the perspective of a young
 1179 geological history. *Anais da Academia Brasileira de Ciências*, 91(4): e20181337.
- 1180 Sana, R. S., Anghinoni, I., Brandão, Z. N., Holzschuh, M. J. (2014). Variabilidade espacial de atributos
 1181 físico-químicos do solo e seus efeitos na produtividade do algodoeiro. *Revista Brasileira de Enge-
 1182 nharia Agrícola e Ambiental*, 18, 994-1002.
- 1183 Sanchez, A. H., Picoli, M. C. A., Camara, G., Andrade, P. R., Chaves, M. E. D., Lechler, S., ..., Queiroz,
 1184 G. R. (2020). Comparison of Cloud cover detection algorithms on sentinel-2 images of the amazon
 1185 tropical forest. *Remote Sensing*, 12(8): 1-16.

- 1186 Sander, C., Gasparetto, N. V. L., Santos, M. L., Carvalho, T. M., Wankler, F. L. (2015a). Aspectos da
 1187 dinâmica morfológica do Alto Rio Branco, adjacências da cidade de Boa Vista, Roraima. In: Gorayeb,
 1188 P. S. S., Lima, A. M. M. (Org.). Contribuições à Geoecologia da Amazônia, 1. ed., v. 9., Belém: SBG
 1189 - Núcleo Norte, p. 15-31.
- 1190 Sander, C., Gasparetto, N., Santos, M. (2015b). Variações da carga sedimentar de fundo e morfologia
 1191 dos perfis transversais batimétricos no trecho inferior da bacia do Alto rio Branco, Roraima. Revista
 1192 Geográfica Acadêmica, 9(1), 130-145.
- 1193 Sander, C., Wankler, F. L., Evangelista, R. A. O., Santos, M. L., Quinonez Fernandez, O. V. (2012).
 1194 Intervenções antrópicas em canais fluviais em áreas urbanizadas: rede de drenagem do Igarapé
 1195 Caranã, Boa Vista-RR. Acta Geográfica, 6(12): 59-84.
- 1196 Sander, C., Wankler, F. L., Tonello, M. F., Sousa, V. P. (2008). Levantamento hidrológico da bacia do
 1197 igarapé Carrapato, Boa Vista, RR: dados preliminares. Acta Geográfica, 2(3), 119-129.
- 1198 Santos, Â. C. S., Holanda, E. C., Souza, V., Guerra-Sommer, M., Manfroi, J., Uhl, D., Jasper, A. (2016).
 1199 Evidence of palaeo-wildfire from the upper lower Cretaceous (Serra do Tucano Formation, Aptian–
 1200 Albian) of Roraima (North Brazil). Cretaceous Research, 57, 46-49.
- 1201 Santos, N. M. C., Vale Junior, J. F., Barbosa, R. I. (2013). Florística e estrutura arbórea de ilhas de
 1202 mata em áreas de savana do norte da Amazônia brasileira. Boletim do Museu Paraense Emílio
 1203 Goeldi-Ciências Naturais, 8(2), 205-221.
- 1204 Shao, Z., Wu, W., Guo, S. (2020). IHS-GTF: A fusion method for optical and synthetic aperture radar
 1205 data. Remote Sensing, 12(17): 2796.
- 1206 Shimabukuro, Y. E., Ponzoni, F. J. (2017). Mistura Espectral: modelo linear e aplicações. Rio de Ja-
 1207 neiro: Oficina de Textos, 1a. Ed., 87 pp.
- 1208 Shipley, B. (2016). Cause and Correlation in Biology: A User's Guide to Path Analysis, Structural Equa-
 1209 tions and Causal Inference with R. Cambridge: Cambridge University Press, 2th. Ed., 314pp.
- 1210 Silva, D. A. D., Klink, C. A. (2001). Dinâmica de foliação e perfilhamento de duas gramíneas C4 e uma
 1211 C3 nativas do Cerrado. Brazilian Journal of Botany, 24: 441-446.
- 1212 Silva, M. G., Porsani, M. J. (2006). Aplicação de balanceamento espectral e DMO no processamento
 1213 sísmico da Bacia do Tacutu. Revista Brasileira de Geofísica, 24(2), 273-290.
- 1214 Silva, D. A., Nascimento, F. A., Silva, L. D., Neta, L. C. B., Júnior, S. S. T. (2010). Características
 1215 Geomorfológicas e a Atuação Antrópica na Formação da Atual Paisagem em Boa Vista, Bonfim e
 1216 Pacaraima. Acta Geográfica, 3(6): 55-64.
- 1217 Silva, F. B., Shimabukuro, Y. E., Aragao, L. E., Anderson, L. O., Pereira, G., Cardozo, F., Arai, E. (2013).
 1218 Large-scale heterogeneity of Amazonian phenology revealed from 26-year long AVHRR/NDVI time-
 1219 series. Environmental Research Letters, 8(2), 024011.
- 1220 Silva, L. J. D., Dick, D. P., Neckel, D., Nóbrega, G. N., Rodrigues, R. D. A. R., Barbosa, R. I., Cordeiro,
 1221 R. C. (2022). Effects of fire on soil organic matter in northern Amazonian forest fragments. Acta
 1222 Amazonica, 52: 13-22.
- 1223 Silveira, H. L. F., Galvão, L. S., Sanches, I. D. A., de Sá, I. B., Taura, T. A. (2018). Use of MSI/Sentinel-
 1224 2 and airborne LiDAR data for mapping vegetation and studying the relationships with soil attributes
 1225 in the Brazilian semi-arid region. International Journal of Applied Earth Observation and Geoinfor-
 1226 mation, 73: 179-190.
- 1227 Silvertown, J., Dodd, M. E., Gowing, D. J., Mountford, J. O. (1999). Hydrologically defined niches reveal
 1228 a basis for species richness in plant communities. Nature, 400(6739): 61-63.
- 1229 Silvertown, J., Araya, Y., Gowing, D. (2015). Hydrological niches in terrestrial plant communities: a re-
 1230 view. Journal of Ecology, 103(1): 93-108.
- 1231 Simões, S. M. O., Zilli, J. É., Costa, M. C. G., Tonini, H., Balieiro, F. D. C. (2010). Carbono orgânico e
 1232 biomassa microbiana do solo em plantios de *Acacia mangium* no Cerrado de Roraima. Acta Ama-
 1233 zonica, 40(1): 23-30.

- 1234 Souza, V., Vieira, C. E. L., Costa, J. A. V., Matos, S. C., Soares, V. M. A. (2010). Ocorrência de Lenhos
1235 Fósseis na Bacia do Tacutu-Roraima. *Acta Geográfica*, 3(5): 73-77.
- 1236 Souza, A. A., Galvão, L.S., Korting, T. S., Prieto, J.D. (2020). Dynamics of savanna clearing and land
1237 degradation in the newest agricultural frontier in Brazil. *Geoscience and Remote Sensing*, 57(7):
1238 965-984.
- 1239 Souza Filho, P. W. M., Paradella, R. W. (2005). Use of RADARSAT-1 fine mode and Landsat-5 TM
1240 selective principal component analysis for geomorphological mapping in a macrotidal mangrove
1241 coast in the Amazon Region. *Canadian Journal of Remote Sensing*, 31(3): 214-224.
- 1242 Sullivan, M. J., Lewis, S. L., Affum-Baffoe, K., Castilho, C., Costa, F., Sanchez, A. C., Vargas, P. N.
1243 (2020). Long-term thermal sensitivity of Earth's tropical forests. *Science*, 368(6493): 869-874.
- 1244 Tadono, T., Ishida, H., Oda, F., Naito, S., Minakawa, K., Iwamoto, H. (2014). Precise global DEM gen-
1245 eration by ALOS PRISM. *ISPRS Annals of the Photogrammetry, Remote Sensing and Spatial Infor-
1246 mation Sciences*, 2(4): 71-76.
- 1247 Tao, S., Guo, Q., Li, C., Wang, Z., Fang, J. (2016). Global patterns and determinants of forest canopy
1248 height. *Ecology*, 97(12): 3265-3270.
- 1249 Vale Júnior, J. F. D., Sousa, M. I. L., Barbosa, R. I., Xaud, H. A. M., Souza, J. M. C. (2005). Savanas
1250 de Roraima: Etnoecologia, biodiversidade e potencialidades agrosilvopastoris. Boa Vista, FEMACT,
1251 2005. p.79-91.
- 1252 Vale Júnior, J. F. D., Schaefer, C.E.G.R. (2010). Guia de solos sob savanas de Roraima. Boa Vista.
1253 Ioris, 219 p.
- 1254 Vale Júnior, J. F. D., Sousa, M. I. L., Nascimento, P. P. R. R. (2014). Solos e Ambientes. In: Holanda,
1255 J. L. R., Marmos, J. L., Maia, M. A. M. (Org.). *Geodiversidade do Estado de Roraima*, 1. ed., Manaus:
1256 CPRM, p. 65–86.
- 1257 Hammen, T., Burger, D. (1964). Pollen flora and age of the Takutu Formation (Guyana). *Leidse Geolo-
1258 gische Mededelingen*, 38: 173-180.
- 1259 Vaz, P. T., Wanderley Filho, J. R., Bueno, G. V. (2007). Bacia do Tacutu. *Boletim de Geociências da
1260 Petrobras*, Rio de Janeiro, 15(2): 289-297.
- 1261 Veenendaal, E. M., Torello-Raventos, M., Feldpausch, T. R., Domingues, T. F., Gerard, F., Schrodt, F.,
1262 ... Lloyd, J. (2015). Structural, physiognomic and above-ground biomass variation in savanna–forest
1263 transition zones on three continents—how different are co-occurring savanna and forest formations?
1264 *Biogeosciences*, 12(10): 2927-2951.
- 1265 Veras, A. T. R., Galdino, L. K. A., Oliveira Jr, Z. (2018). Occupation of urban space and legal evolution
1266 of the app's of the water courses of Law No. 12.651/2012: temporal reflections in the city of Boa
1267 Vista-Roraima. *Direito da Cidade*, 10(3): 1761-1788.
- 1268 Villalobos-Vega, R., Salazar, A., Miralles-Wilhelm, F., Haridasan, M., Franco, A. C., Goldstein, G.
1269 (2014). Do groundwater dynamics drive spatial patterns of tree density and diversity in Neotropical
1270 savannas? *Journal of vegetation science*, 25(6), 1465-1473.
- 1271 Walker, B. H. (1987). Determinants of Tropical Savannas. Oxford, UK: IRL Press Ltd., 1st. ed., 167 pp.
- 1272 Wankler, F. L., Evangelista, R. A. O. Sander, C. (2012). Sistema Aquífero Boa Vista: "Estado da Arte"
1273 do conhecimento e perspectivas. *ACTA Geográfica*, Boa Vista, 6(12): 21-39.
- 1274 Ward, D. P., Petty, A., Setterfield, S. A., Douglas, M. M., Ferdinand, K., Hamilton, S. K., Phinn, S.
1275 (2014). Floodplain inundation and vegetation dynamics in the Alligator Rivers region (Kakadu) of
1276 northern Australia assessed using optical and radar remote sensing. *Remote Sensing of Environ-
1277 ment*, 147: 43-55.
- 1278 Xaud, M. R., Xaud, H. A. M., Ferreira, N. J., Kampel, M., Santos, J. R. (2009). Análise de padrões de
1279 vegetação através de séries temporais de NDVI-NOAA e suas relações com o clima em Roraima.
1280 *Anais XIV Simpósio Brasileiro de Sensoriamento Remoto*, Natal, Brasil. INPE, p. 3143-3150

- 1281 Xaud, H. A. M., Carvalho, V. C. (1999). Definição de unidades de paisagem natural através de cruza-
1282 mentos entre mapas: abordagem crítica e aplicabilidade. In: Congresso e Feira para Usuários de
1283 Geoprocessamento da América Latina, 5, Salvador. Anais... Salvador: INPE. p.1-18.
- 1284 Zalán, P. V. (2004). Evolução fanerozóica das bacias sedimentares brasileiras. In: Geologia do Conti-
1285 nente Sul-Americano: Evolução da obra de Fernando Flávio Marques de Almeida. São Paulo, Beca:
1286 595-613.
- 1287 Zani, H., Rossetti, D. F. (2012). Multitemporal Landsat data applied for deciphering a megafan in north-
1288 ern Amazonia. International Journal of Remote Sensing, 33(19), 6060-6075.
- 1289 Zular, A., Sawakuchi, A. O., Chiessi, C. M., d'Horta, F. M., Cruz, F. W., Demattê, J. A. M., ... Soares, E.
1290 A. A. (2019). The role of abrupt climate change in the formation of an open vegetation enclave in
1291 northern Amazonia during the late Quaternary. Global and planetary change, 172, 140-149.
- 1292 Zuquim, G., Tuomisto, H., Jones, M. M., Prado, J., Figueiredo, F. O., Moulatlet, G. M., ..., Emilio, T.
1293 (2014). Predicting environmental gradients with fern species composition in Brazilian Amazonia.
1294 Journal of Vegetation Science, 25(5), 1195-1207.
- 1295 Zuquim, G., Costa, F. R., Tuomisto, H., Moulatlet, G. M., Figueiredo, F. O. (2020). The importance of
1296 soils in predicting the future of plant habitat suitability in a tropical forest. Plant and Soil, 450(1), 151-
1297 170.

2.1 NORMAS DA REVISTA

Manuscrito elaborado para submissão ao periódico *Remote Sensing of Environment*. A escolha desse periódico deve-se ao seu alto fator de impacto interdisciplinar, não apenas no âmbito do sensoriamento remoto, mas também das ciências ambientais, geociências e biodiversidade. Guia aos autores em: <https://www.elsevier.com/journals/remote-sensing-of-environment/0034-4257/guide-for-authors>.

3 CONCLUSÃO

Na área estudada, o vigor da vegetação variou consideravelmente tanto em termos espaciais (77%), quanto temporais (>60%), ou seja, por um lado as diferenças de NDVI registradas dentro da área variaram desde a completa ausência de qualquer tipo de vegetação, até densas manchas florestais e, por outro lado, quando comparadas imagens de distintas épocas, houve também uma significativa variação do NDVI, particularmente quando se comparam imagens de épocas de chuvas com épocas de secas.

Considerando-se que de todos os caracteres abióticos aqui analisados, apenas a precipitação e a temperatura têm a capacidade de variar significativamente nas escalas de tempo analisadas, é possível atribuir à precipitação grande parte da responsabilidade por esta variação. De fato, os resultados do Modelo de Equações Estruturadas apontaram um efeito positivo significativo no NDVI da precipitação (0,23) e um efeito secundário e inverso da temperatura (-0,11). A precipitação variou mais no tempo (0,95%) do que no espaço (30%). Dado o caráter xeromórfico da vegetação de savana, a maior proximidade a corpos d'água perenes explica a variação espacial e o aporte de água durante as épocas de chuva explica a variação temporal.

Essa influência, no entanto, não é linear, pois em casos onde as chuvas geram acumulações expressivas de água, a concomitante ausência de ar nos poros dos solos decorrente da sua saturação pode afogar as raízes e matar as plantas, exercendo assim, um efeito negativo no NDVI. De fato, inundações mostraram efeitos negativos na vegetação (-0,15), ainda que não tão elevados quanto o esperado.

Para a savana roraimense, a altitude e a declividade do terreno não se mostraram muito importantes para o comportamento e distribuição da savana, ao contrário da geologia e da geomorfologia, cujos efeitos indiretos no NDVI da vegetação foi de 0,33 e 0,16, respectivamente. O maior valor da geologia deve-se a dois fatos, o primeiro, de que ela é a fonte primária da química das partículas minerais dos solos, e o segundo, de que a geomorfologia foi ordenada pela altitude.

Os solos se fazem mais influentes quanto ao seu grau de compactação, conforme pode-se observar pela magnitude do efeito obtido para a Densidade Aparente (-0,37). Os valores para a CEC, Areia e SOCS foram, respectivamente, -

0,27, 0,15 e -0,09. É fácil entender o resultado da Densidade Aparente, já que, quanto maior ela for, menor será a capacidade de infiltração do solo e maior será o escoamento superficial, implicando que, após cessada a chuva, as plantas podem ter dificuldade de obter a água necessária, quer porque a água já tenha escoado, quer porque suas raízes não conseguem receber ou capturar água no solo impermeabilizado.

Por outro lado, esperava-se uma influência positiva da CEC, relativa a capacidade do solo trocar cátions importantes ao desenvolvimento vegetal. Sua influência negativa deve-se ao fato de que muitos solos da savana roraimense costumam apresentar altas concentrações de cátions de alumínio, tóxicos ao desenvolvimento vegetal. O efeito positivo da concentração de areia reforça as restrições hidroedáficas da região, áreas periodicamente inundadas dificultam o estabelecimento de espécies de árvores, o que é favorecido em áreas com melhores condições de drenagem.

REFERÊNCIAS

ALIX-GARCIA, J.; GIBBS, H. K. Forest conservation effects of Brazil's zero deforestation cattle agreements undermined by leakage. **Global Environmental Change**, Amsterdam, v. 47, p. 201-217, nov. 2017.

ALVES, D.B.; PÉREZ-CABELLO, F. Multiple remote sensing data sources to assess spatio-temporal patterns of fire incidence over Campos Amazônicos Savanna Vegetation Enclave (Brazilian Amazon). **Science of the Total Environment**, Amsterdam, v. 601-6021, p. 142-158, dez. 2017.

ARAÚJO JÚNIOR, A. C. R.; TAVARES JÚNIOR, S. S. Land use and cover for urban planning, Boa Vista, Roraima, Brasil. **Boletim Goiano de Geografia**, Goiana, v. 37, n. 1, p. 36-55, jan-abr. 2017.

BANERJEE, O.; CICOWIEZ, M.; MACEDO, M.; MALEK, Z.; VERBURG, P. H.; GOODWIN, S.; VARGAS, R.; RATTIS, L.; BRANDO, P. M.; COE, M. T.; NEIL, C.; MARTI, O. D. An Amazon Tipping Point: The Economic and Environmental Fallout. **IDB Working Paper Series** N° IDB-WP-01259, 107 pp. 2021.

BARBER, C.P.; COCHRANE, M. A.; SOUZA JR., C. M.; LAURENCE, W. F. Roads, deforestation, and the mitigating effect of protected areas in the Amazon. **Biological Conservation**, Amsterdam, v. 177, p. 203-209, set. 2014.

BARBOSA, R. I.; CAMPOS, C.; PINTO, F.; FEARNSIDE, P. M. The "Lavrados" of Roraima: biodiversity and conservation of Brazil's Amazonian Savannas. **Functional Ecosystems and Communities**, Tokyo, v. 1, n. 1, p. 29-41, jan. 2007.

BARBOSA, R. I.; CAMPOS, C. Detection and geographical distribution of clearing areas in the savannas ('Lavrado') of Roraima using Google Earth web tool. **Journal of Geography and Regional Planning**, London, v. 4, n. 3, p. 122-136, fev. 2011.

BARBOSA, R. I.; FEARNSIDE, P.M. Above-ground biomass and the fate of carbon after burning in the savannas of Roraima, Brazilian Amazonia. **Forest Ecology and Management**, Amsterdam, v. 216, n. 1-3, p. 295-316, dez. 2005a.

BARBOSA, R. I.; FEARNSIDE, P.M. Fire frequency and area burned in the Roraima savannas of Brazilian Amazonia. **Forest Ecology and Management**, Amsterdam, v. 204, n. 2-3, p. 371-384, jan. 2005.

BARBOSA, R. I.; MIRANDA, I. D. S. Fitofisionomias e diversidade vegetal das savanas de Roraima. In: BARBOSA, R. I.; XAUD, H. A. M.; COSTA E SOUZA, J. M. (ORG.). **Savanas de**

Roraima: Etnoecologia, Biodiversidade e Potencialidades Agrossilvipastoris. 1 ed. Boa Vista: FEMACT, 2005. p. 61-78.

BARNI, P.E.; FEARNSIDE, P.M.; GRAÇA, P.M.L.A. Deforestation and Carbon Emissions in Amazonia: Simulating the Impact of Connecting Brazil's State of Roraima to the "Arc of Deforestation" by Reconstructing the BR-319 (Manaus-Porto Velho) Highway. In: XII Congreso Forestal Mundial, 12., 2009, Buenos Aires. **Anais...** Buenos Aires: UBA, 2009. p. 1-16.

BARNI, P. E.; PEREIRA, V. B.; MANZI, A. O.; BARBOSA, R. I. Deforestation and forest fires in Roraima and their relationship with phytoclimatic regions in the Northern Brazilian Amazon. **Environmental Management**, Berlin, v. 55, n. 5, p. 1124-1138, jan. 2015.

CARVALHO, W.D.; MUSTIN, K.; HILÁRIO, R.R.; VASCONCELOS, I.M.; EILERS, V.; FEARNSIDE, P.M. Deforestation control in the Brazilian Amazon: A conservation struggle being lost as agreements and regulations are subverted and bypassed. **Perspectives in Ecology and Conservation**, Amsterdam, v. 17, n. 3, p. 122–130, jul-set. 2019.

CARVALHO, W. D.; MUSTIN, K. The highly threatened and little known Amazonian savannahs. **Nature Ecology & Evolution**, California, v. 1, n. 4, p. 1-3, mar. 2017.

DEVECCHI, M. F., LOVO, J., MORO, M. F., ANDRINO, C. O., BARBOSA-SILVA, R. G., VIANA, P. L., ...; ZAPPI, D. C. Beyond forests in the Amazon: biogeography and floristic relationships of the Amazonian savannas. **Botanical Journal of the Linnean Society**, Oxford, v. 193, n. 4, p. 478-503, ago. 2020.

DINIZ, A.M.A.; LACERDA, E.G. The Colonization of Roraima State, Brazil: an Analysis of its Major Migration Flows (1970 to 2010). **Espace Populations Sociétés**, Paris, v. 2-3, p. eps5817, jul. 2014.

DINIZ, A.M.A.; LACERDA, E.G. The complexities of the Brazilian Amazon frontier and its most recent chapter: soybean expansion in Roraima. In.: JONES, R.; DINIZ, A. M. A. (Org.). **Twentieth Century Land Settlement Schemes**, 1 ed. Nova York: Routledge, 2018. p. 178-204.

DONG, X.; LI, F.; LIN, Z.; HARRISON, S.P.; CHEN, Y.; KUNG, J.-S. Climate influence on the 2019 fires in Amazonia. **Science of The Total Environment**, Amsterdam, v. 794, p. 148718, dez. 2021.

DURIGAN, G.; RATTER, J.A. The need for a consistent fire policy for Cerrado conservation. **Journal of Applied Ecology**, London, v. 53, n. 1, p. 11-15, out. 2015.

FEARNSIDE, P.M. Highway construction as a force in the destruction of the Amazon Forest. In.: REE, R.; SMITH, D. J.; GRILO, C. (Org.). **Handbook of Road Ecology**, 1 ed., Nova York: John Wiley and Sons Ltd., 2015. p. 414-424.

FERNANDES, G.W.; COELHO, M.S.; MACHADO, R.B.; FERREIRA, M.E.; AGUIAR, L.M.S.; DIRZO, R.; SCARIOT, A.; LOPES, C.R. Afforestation of savannas: an impending ecological disaster. **Brazilian Journal of Nature Conservation**, Rio de Janeiro, v. 14, p. 146-151, mar. 2016.

FERRANTE, L.; FEARNSIDE, P.M. Brazil's new president and 'ruralists' threaten Amazonia's environment, traditional peoples and the global climate. **Environmental Conservation**, Cambridge, v. 46, n. 4, p. 261 –263, dez. 2019.

FLORES, B.M.; DECHOUUM, M.S.; SCHMIDT, I.B.; HIROTA, M.; ABRAHÃO, A.; VERONA, L.; PECORAL, L.L.F.; CURE, M.B.; GILES, A.L.; COSTA, P.B.; PAMPLONA, M.B.; MAZZOCHINI, G.G.; GROENENDIJK, P.; MINSKI, G.L.; WOLFSDORF, G.; SAMPAIO, A.B.; PICCOLO, F.; MELO, L.; LIMA, R.F.; OLIVEIRA, R.S. Tropical riparian forests in danger from large savanna wildfires. **Journal of Applied Ecology**, London, v. 58, n. 2, p. 419-430, 2021.

FURLAN, L. M., ROSOLEN, V., SALLES, J., MOREIRA, C. A., FERREIRA, M. E., BUENO, G. T., ...; MOUNIER, S. Natural superficial water storage and aquifer recharge assessment in Brazilian savanna wetland using unmanned aerial vehicle and geophysical survey. **Journal of Unmanned Vehicle Systems**, Ottawa, v. 8, n. 3, p. 224-244, set. 2020.

FURLEY, P.A. **The Forest Frontier**. 1 ed. London: Routledge, 1994. 260 p.
GIBBS, H.K.; RAUSCHA, L.; MUNGER, J.; SCHELLY, I.; MORTON, D.C.; NOOJIPADY, P.; SOARES-FILHO, B.; BARRETO, P.; MICOL, L.; WALKER, N.F. Brazil's Soy Moratorium. **Science**, Washington, v. 347, n. 6220, p. 377-378, jan. 2015.

GOMES, L.; MIRANDA, H.S.; SOARES-FILHO, B.; RODRIGUES, L.; OLIVEIRA, U.; BUSTAMANTE, M.M.C. Responses of Plant Biomass in the Brazilian Savanna to Frequent Fires. **Frontiers in Forest and Global Change**, Lausanne, v. 24, p. 1-11, nov. 2020.

HOEVE, J.E.T.; REMER, L.A.; CORREIA, A.L; JACOBSON, M.Z. Recent shift from forest to savanna burning in the Amazon Basin observed by satellite. **Environmental Research Letters**, Bristol, v. 7, p. 024020, jun. 2012.

IBGE. **Manual Técnico da Vegetação Brasileira**. 1 ed. Rio de Janeiro: IBGE, 2012. 271 p.
KELLEY, D.I.; BURTON, C.; HUNTINGFORD, C.; BROWN, M.A.J.; WHITLEY, R.; DONG, N. Technical note: Low meteorological influence found in 2019 Amazonia fires. **Biogeosciences**, Berlin, v. 126, n. 18, p. 787-804, mar. 2021.

LEHMANN, C. E.; ANDERSON, T. M.; SANKARAN, M.; HIGGINS, S. I.; ARCHIBALD, S.; HOFFMANN, W. A.; ... BOND, W. J. Savanna vegetation-fire-climate relationships differ among continents. **Science**, 1109 343(6170), 548-552, set. 2014.

LIMA, M.S.B. Expansão da cadeia da soja na Amazônia Setentrional: os casos de Roraima e Amapá. **Boletim de Geografia da Universidade Estadual de Maringá**, Maringá, v. 38, n. 2, p. 79-93, out. 2020.

MAPBIOMAS. Statistics. 2022. Disponible in: <https://mapbiomas.org/en/statistics>. Last accessed: 04/19/2022.

MILLER, G. R.; CABLE, J. M.; MCDONALD, A. K.; BOND, B.; FRANZ, T. E.; WANG, L.; ...; SCOTT, R. L. Understanding ecohydrological connectivity in savannas: a system dynamic modelling approach. **Ecohydrology**, Hoboken, v. 5, n. 2, p. 200-220, mai. 2012.

MIRANDA, I. S.; ABSY, M. L. Fisionomia das savanas de Roraima, Brasil. **Acta Amazonica**, Manaus, v. 3, p. 423-440, set. 2000.

MISTRY, J., BERADI, A. (2000). The Savanna ecosystem. In.: MISTRY, J.; BERADI, A. (Org.). **World Savannas - Ecology and Human Use**. 1 ed. Nova York: Routledge, 2000. p. 1-25.

OSBORNE, C. P.; CHARLES- DOMINIQUE, T.; STEVENS, N.; BOND, W. J.; MIDGLEY, G.; LEHMANN, C. E. Human impacts in African savannas are mediated by plant functional traits. **New Phytologist**, Hoboken, v. 220, n. 1, p. 10-24, jan. 2018.

PENNINGTON, R.T.; LEHMANN, C.E.R.; ROWLAND, L.M. Tropical savannas and dry forests. **Current Biology**, Cambridge, v. 28, p. R527-R548, abr. 2018.

RESENDE- MOREIRA, L. C.; KNOWLES, L. L.; THOMAZ, A. T.; PRADO, J. R.; SOUTO, A. P.; LEMOS- FILHO, J. P.; LOVATO, M. B. Evolving in isolation: genetic tests reject recent connections of Amazonian savannas with the central Cerrado. **Journal of Biogeography**, Hoboken, v. 46, n. 1, p. 196-211, jan. 2019.

SCHMIDT, I. B.; ELOY, L. Fire regime in the Brazilian Savanna: Recent changes, policy and management. **Flora**, Amsterdam, v. 268, p. 151613, jul 2020.

SIMIONI, P. F.; EISENLOHR, P. V.; PESSOA, M. J. G.; DA SILVA, I. V. Elucidating adaptive strategies from leaf anatomy: do Amazonian savannas present xeromorphic characteristics?. **Flora**, Amsterdam, v. 226, p. 38-46, jan. 2017.

SOUZA, A. A.; GALVÃO, L.S.; KORTING, T. S.; PRIETO, J.D. Dynamics of savanna clearing and land degradation in the newest agricultural frontier in Brazil. **Geoscience and Remote Sensing**, Nova York, v. 57, n. 7, p. 965-984, ago. 2020.

VACCHIANO, M. C.; SANTOS, J. W.; ANGEOLETTO, F.; SILVA, N. M. Do Data Support Claims That Brazil Leads the World in Environmental Preservation?. **Environmental Conservation**, Cambridge, v. 46, n. 2, p. 118-120, mai. 2019.

VELDMAN, J. W.; BUISSON, E.; DURIGAN, G.; FERNANDES, G. W.; LE STRADIC, S.; MAHY, G.; ...; BOND, W. J. Toward an old- growth concept for grasslands, savannas, and woodlands. **Frontiers in Ecology and the Environment**, Washington, v. 13, n. 3, p. 154-162, out. 2015.

VELDMAN, J.W.; PUTZ, F. E. Grass-dominated vegetation, not species-diverse natural savanna, replaces degraded tropical forests on the southern edge of the Amazon Basin. **Biological Conservation**, Amsterdam, v. 144, n. 5, p. 1419-1429, ago. 2011.

VERAS, A.R.T. **A produção do espaço urbano e Boa Vista – Roraima**. 2009. 235 f. Tese (Doutorado em Geografia) – Universidade de São Paulo, São Paulo, 2009.

VERAS, A.R.T.; GALDINO, L.K.A; OLIVEIRA JR., Z. Occupation of urban space and legal evolution of the APP's of the water courses of law, no. 12.651/2012. **Direito da Cidade**, Rio de Janeiro, v. 10, n. 3, p. 1761+, abr. 2012.

VILLALOBOS- VEGA, R., SALAZAR, A., MIRALLES- WILHELM, F., HARIDASAN, M., FRANCO, A. C., GOLDSTEIN, G. Do groundwater dynamics drive spatial patterns of tree density and diversity in Neotropical savannas? **Journal of vegetation science**, Hoboken, v. 25, n. 6, p. 1465-1473, set. 2014.

WANKLER, F. L.; EVANGELISTA, R. A. O.; SANDER, C. Sistema Aquífero Boa Vista: “Estado da Arte” do conhecimento e perspectivas. **ACTA Geográfica**, Boa Vista, v. 6, n. 12, p. 21-39, ago. 2012.